TYPE IN YOUR DEFAULT TITLE HERE: YOU MAY NEED TO CHANGE THE SPACING IF THE TITLE IS TOO LONG AND PUSHES THE COPYRIGHT OFF OF THE TITLEPAGE

A Dissertation

by

STEVEN ALVARO BOADA

Submitted to the Office of Graduate and Professional Studies of
Texas A&M University
in partial fulfillment of the requirements for the degree of

DOCTOR OF PHILOSOPHY

Chair of Committee,	Casey J. Papovich
Committee Members,	Wolfgang Bangerth
	Louis Strigari
	Nicholas Suntzeff
Head of Department,	George Welch

August 2016

Major Subject: Physics and Astronomy

ABSTRACT

Lorem ipsum dolor sit amet, consectetur adipiscing elit. Integer lectus quam, condimentum quis bibendum eu, sollicitudin eget lacus. Praesent non sodales odio. Class aptent taciti sociosqu ad litora torquent per conubia nostra, per inceptos himenaeos. Nulla ac luctus sapien. Morbi cursus sapien eget lorem fermentum hendrerit. Nam ac erat dui, in cursus velit. Vivamus hendrerit porttitor nisi, ut porttitor lorem volutpat eget. In ligula ligula, euismod ut condimentum sit amet, pulvinar sit amet diam. Pellentesque interdum, ipsum ullamcorper consequat dignissim, sem arcu egestas mauris, vitae interdum sem tortor ut ante. Nunc blandit laoreet nisi, non rutrum lorem hendrerit quis. Cras nunc diam, convallis et feugiat at, auctor id libero. Nunc facilisis massa eu eros imperdiet vestibulum. Vestibulum ante ipsum primis in faucibus orci luctus et ultrices posuere cubilia Curae; Donec non velit vitae tortor blandit semper.

Etiam vitae dolor nulla. Ut eros odio, rhoncus eget placerat vitae, elementum ac ante. Proin vitae odio eu nisl pharetra mattis. Pellentesque habitant morbi tristique senectus et netus et malesuada fames ac turpis egestas. Phasellus fermentum lacus consectetur neque consequat ullamcorper. Cras blandit urna non dui consequat molestie. Curabitur viverra nibh at nisi semper faucibus. Nam egestas mauris a enim dignissim nec consectetur tortor rutrum. Mauris at nisi in est luctus congue ut mattis est. Ut pretium, mi quis elementum cursus, ante eros suscipit ligula, ut porttitor elit leo sed turpis. Nam sed dui ligula.

DEDICATION

This is an optional page. Lorem ipsum dolor sit amet, consectetur adipiscing elit. Integer lectus quam, condimentum quis bibendum eu, sollicitudin eget lacus. Praesent non sodales odio. Class aptent taciti sociosqu ad litora torquent per conubia nostra, per inceptos himenaeos. Nulla ac luctus sapien. Morbi cursus sapien eget lorem fermentum hendrerit. Nam ac erat dui, in cursus velit. Vivamus hendrerit porttitor nisi, ut porttitor lorem volutpat eget. In ligula ligula, euismod ut condimentum sit amet, pulvinar sit amet diam. Pellentesque interdum, ipsum ullamcorper consequat dignissim, sem arcu egestas mauris, vitae interdum sem tortor ut ante. Nunc blandit laoreet nisi, non rutrum lorem hendrerit quis. Cras nunc diam, convallis et feugiat at, auctor id libero. Nunc facilisis massa eu eros imperdiet vestibulum. Vestibulum ante ipsum primis in faucibus orci luctus et ultrices posuere cubilia Curae; Donec non velit vitae tortor blandit semper.

Etiam vitae dolor nulla. Ut eros odio, rhoncus eget placerat vitae, elementum ac ante. Proin vitae odio eu nisl pharetra mattis. Pellentesque habitant morbi tristique senectus et netus et malesuada fames ac turpis egestas. Phasellus fermentum lacus consectetur neque consequat ullamcorper. Cras blandit urna non dui consequat molestie. Curabitur viverra nibh at nisi semper faucibus. Nam egestas mauris a enim dignissim nec consectetur tortor rutrum. Mauris at nisi in est luctus congue ut mattis est. Ut pretium, mi quis elementum cursus, ante eros suscipit ligula, ut porttitor elit leo sed turpis. Nam sed dui ligula.

ACKNOWLEDGEMENTS

Lorem ipsum dolor sit amet, consectetur adipiscing elit. Integer lectus quam, condimentum quis bibendum eu, sollicitudin eget lacus. Praesent non sodales odio. Class aptent taciti sociosqu ad litora torquent per conubia nostra, per inceptos himenaeos. Nulla ac luctus sapien. Morbi cursus sapien eget lorem fermentum hendrerit. Nam ac erat dui, in cursus velit. Vivamus hendrerit porttitor nisi, ut porttitor lorem volutpat eget. In ligula ligula, euismod ut condimentum sit amet, pulvinar sit amet diam. Pellentesque interdum, ipsum ullamcorper consequat dignissim, sem arcu egestas mauris, vitae interdum sem tortor ut ante. Nunc blandit laoreet nisi, non rutrum lorem hendrerit quis. Cras nunc diam, convallis et feugiat at, auctor id libero. Nunc facilisis massa eu eros imperdiet vestibulum. Vestibulum ante ipsum primis in faucibus orci luctus et ultrices posuere cubilia Curae; Donec non velit vitae tortor blandit semper.

Etiam vitae dolor nulla. Ut eros odio, rhoncus eget placerat vitae, elementum ac ante. Proin vitae odio eu nisl pharetra mattis. Pellentesque habitant morbi tristique senectus et netus et malesuada fames ac turpis egestas. Phasellus fermentum lacus consectetur neque consequat ullamcorper. Cras blandit urna non dui consequat molestie. Curabitur viverra nibh at nisi semper faucibus. Nam egestas mauris a enim dignissim nec consectetur tortor rutrum. Mauris at nisi in est luctus congue ut mattis est. Ut pretium, mi quis elementum cursus, ante eros suscipit ligula, ut porttitor elit leo sed turpis. Nam sed dui ligula.

NOMENCLATURE

B/CS	Bryan/College Station
HSUS	Humane Society of the United States
P	Pressure
T	Time
TVA	Tennessee Valley Authority
TxDOT	Texas Department of Transportation

This page is optional.

TABLE OF CONTENTS

Page

LIST OF FIGURES

FIGURE Page

LIST OF TABLES

TABLE Page

1. INTRODUCTION: THE IMPORTANCE OF RESEARCH

*

Clusters of galaxies form the largest bound objects in the universe, and as such their study is a cornerstone in modern day astronomy. First recognized by 19th century astronomers, their place in astronomical canon was solidified when Edwin Hubble proofed their constituent nebulae where not bound to the Milky Way (Hubble, 1926) but collections of stars similar to the Milky Way. Work to understand their nature and origin began in ernest when Hubble and Humason (1931) used the virial theorem and the galaxy velocities in the centers of the Virgo (Smith, 1936) and Coma (Zwicky, 1933) clusters to derive their masses. The immense mass derived exceeded the total stellar mass contributed by all galaxies many times over. This lead Zwicky to theorize the existence of large amounts of non-luminous matter, and coining the term "dark matter" (DM), which we still use today.

Modern astronomy gives the composition of galaxy clusters in three many parts. The galaxies themselves comprise the most obvious feature, and contain a large portion (but not the entirety) of the luminous matter (stars) in the cluster. The intracluster medium (ICM) is the space between the cluster galaxies and is composed many of ordinary matter (baryons) which are super heated to tens of thousands of kelvin. The ICM contains the bulk of the cluster's baryonic matter, and while it is very hot, it is not very dense, with a typical value of 10^{-3} particles per cubic centimeter. The majority of the cluster's mass is located in the DM halo which surrounds the cluster.

Thought to form out of the primordial density fluctuations in the very early universe, the investigation of their formation and growth began in the 1960s. Soon thereafter, the hierarchical model of structure formation (Press and Schechter, 1974; Gott and Rees, 1975; White and Rees, 1978) was introduced. It suggests the first stars and stellar clumps grew first then subsequently merged together with dark matter and other gas clumps to form the first galaxies which then continued to merge and grow into the clusters and large scale structures we see today. This accretion of smaller systems is thought to be driven by the gravity of the DM associated with the cluster. Of course, many complicated astrophysical processes are at work during cluster growth and similarly complicated theoretical models seek to explain these processes. For a detailed review of cluster formation see Kravtsov and Borgani (2012).

The number and distribution of galaxy clusters across the sky is the finger print of the cosmology imprinted on the universe at its birth. To uncover the underlying cosmology a detailed understanding of the astrophysical processes that describe the motion of constituent galaxies and their impact on the ICM is required. So, galaxy clusters stand at the intersection of cosmology and astrophysics.

1.1 Cluster Cosmology

The current concordance cosmology is a parametrization of the Big Bang cosmological model where the universe contains a cosmological constant (Λ; often referred to as dark energy) and cold dark matter (CDM). It is often characterized by six parameters; the Hubble Constant (H_0), the baryonic matter density (Ω_b), the dark matter density (Ω_c), the dark energy density (Ω_Λ); the normalization of the power spectrum (σ_8); the spectral index of the power spectrum (n_s). Galaxy clusters are sensitive probes of Ω_m, the total mass ($\Omega_b + \Omega_c$) density in the universe, through

tracing the peaks in the universal matter density often referred to as the power spectrum of matter density fluctuations or the matter power spectrum and σ_8 by the comparison of the number density of observed halos to that predicted in cosmological models.

The determination of cosmological parameters is done by comparing the number of galaxy clusters per unit mass per unit comoving volume ($n(M, z)$) to models. See Allen et al. (2011) for a comprehensive review or Murray et al. (2013) for a more practical approach. $n(M, z)$, referred to as the halo mass function (HMF) captures the number evolution through a function which defines the particular model used. Early work by Press and Schechter (1974) and Bond et al. (1991) which assumed spherical halos, have largely been replaced by more modern fitting functions which, at the expense of an analytical solution, provide more accurate results when fit to simulation data. See Murray et al. (2013) for a review of the most common fitting functions used. Through this approach, the two parameters which clusters are most sensitive to, Ω_m and σ_8 are in reality measured as $\sigma_8\Omega_m^\alpha$, where the value of α depends on the masses of the halos considered. The degeneracy is broken through the evolution of the HMF as a function of redshift.

The ΛCDM model of cosmology makes explicit predictions about the number and masses of galaxy clusters throughout the universe. Connecting these predictions to a set of, sufficiently large in size, observed clusters remains a principal problem. Specifically, the largest threat to modern, precision, cluster cosmology is not the identification of large numbers of clusters (the total number of clusters known is only going up) but the accurate recovery of galaxy cluster mass. This problem extends to both the very rich clusters (those with high mass) and, importantly, the poor clusters (those with low mass) as the relationship between galaxy cluster mass and many of the observables which trace mass is not well understood for such low

mass clusters.

1.2 State of Play

As mass is not a direct observable, a lot of work is underway to characterize galaxy cluster masses with an observable feature of galaxy clusters. In this section, we will briefly touch on a few of the ways cluster mass is determined, and address any short comings the method may have. Generally, the methods fall into two distinct camps, simulation based and direct or statistical calibration. The goal is to constrain, as best possible, $P(X|M,z)$ or the probability (P) that a galaxy cluster of given mass (M) located at redshift (z) using observable parameter (X).

One could use various simulations to attempt to calibrate this observable–mass relation (e.g., Vanderlinde et al. 2010; Sehgal et al. 2011). However, the primary challenge to this method is the incomplete understanding of the baryonic physics which take place in galaxy cluster environments. While there have been (and continue to be) many improvements in the accuracy and power of simulations it is doubtful that in the coming years they will reach the accuracy level required to the point where the observable–mass relation is dominated only by statistics (Weinberg et al., 2013).

The second broad camp is the direct calibration of cluster masses. This recipe has two distinct but not always independent tracks. The "direct" method uses the direct observations of a small set of clusters and then uses known mass estimators, X-ray hydrostatic or weak lensing (WL) as examples, which provide a "true" mass. This directly calibrates the observable–mass relation which is then applied to a much larger sample. The complications lie in that the "true" masses are in fact estimations, and the methods used to recover these masses are subject to their own limitations. X-ray hydrostatic estimations assume hydrostatic equilibrium (e.g., Mantz et al.

2015) which may only be valid for a very small number and range of cluster masses. The Sunyaev–Zeldovich (SZ; Sunyaev and Zeldovich 1972) effect, which uses the up–scattering of cosmic microwave background (CMB) photons to estimate cluster masses, provides accurate estimations of mass, but the ability to detect low mass galaxy clusters is currently limited by technology (e.g., Carlstrom et al. 2002). WL estimates are, in principle, correct in the mean, but they suffer from signal-to-noise requirements, limiting their usefulness in low mass clusters, and potentially suffer from line-of-sight effects as the effect is sensitive to all mass along the line of sight. Virial mass estimators which determine the cluster mass based on the motions of the member galaxies is promising in that it is a direct measurement of the depth of clusters potential well, but suffers from systematics due to cluster formation physics which disrupts the velocity field.

The statistical method of determining galaxy cluster mass relies not on direct measurements of individual clusters but the calibration of observables for the entire sample which correlate with cluster mass. One example is the spatial clustering of the galaxy clusters themselves. See Weinberg et al. (2013) for a comprehensive review. In practice, it will be a combination of the three methods touched on that will provide the most reliable determination of cluster masses.

Virial mass estimators, specifically, can be applied in both a direct and statistical fashion. Currently, the accuracy of such a method, especially to the level required for today's precision cosmology, is not well constrained. In the coming years large spectroscopic surveys will provide enough coverage, and so these methods warrant further investigation (e.g., Saro et al. 2013).

1.3 Cluster Surveys in the near-future

In the coming years, many large surveys will add further statistical advantages to the determination of cosmological parameters using galaxy clusters. At their completion, the South Pole Telescope (SPT; Carlstrom et al. 2011) and the Atacama Cosmology Telescope (ACT; Swetz et al. 2011) are expected to find approximately one thousand clusters using observations in the millimeter combined with the SZ effect. Attempts are already underway to calibrate these observations using subsamples of clusters (approximately 100 cluster candidates and 60 clusters respectively) and other observables such as virial estimates or X-ray temperature measurements (e.g., Sifón et al. 2013; Bocquet et al. 2015).

X-ray identified clusters, up until today, have mostly been observed fortuitously through targeted *Chandra* or *XMM-Newton* observations. That is soon to change with the *eROSITA* telescope onboard the Spektrum-Roentgen-Gamma Mission, which will perform an all–sky survey during its four year mission and detect an estimated 50,000 or more clusters.

Large optical surveys such as the Dark Energy Survey (DES; The Dark Energy Survey Collaboration 2005) and the Large Synoptic Survey Telescope (LSST) will survey enormous portions of the sky extremely deeply and will identify vast numbers of clusters using optical selection methods (e.g., Rykoff et al. 2014; **?**). However, the majority of these surveys will be photometric, and any spectral information will be obtained from preexisting datasets. And while it is possible to estimate cluster masses using photometric redshifts, primarily through the richness–mass relation, (e.g., Rykoff et al. 2012, 2014), spectroscopic followup is required to both better calibrate the relation and to obtain the level of precision needed to compete with other mass estimators.

1.3.1 Impact of This Work

As the sample of known clusters grows to many tens of thousands, spectroscopic followup becomes unfeasible. Large spectroscopic surveys will be required to reduce systematics to a level that will allow accurate mass estimations using virial methods. The Hobby Eberly Dark Energy Experiment (HETDEX; Hill et al. 2008a) is a forthcoming blind spectroscopic survey that could potentially be used to accurately calibrate the observable–mass relation for a significant number of galaxy clusters at both extremes of the mass scale. HETDEX is designed to measure the dark energy equation of state at $z \sim 2$, and so the applicability to galaxy cluster science has not yet been investigated.

Given how much progress could be made with HETDEX, this work seeks to address this issue in two ways. First, using a set of state-of-the-art simulations we will simulate the observing strategy of HETDEX to determine the number and nature of clusters that might be observed. See Section **??**. This is done in four distinct ways and in each part we will measure the dynamical properties, such as redshift, LOSVD, and mass of the clusters. First we will use targeted observations and perfect knowledge of the observed galaxy clusters, which includes center, membership, and number to recover the desired properties. Secondly, we will assume that we know the location but not the center, membership, or number of constituent galaxies. Then we will employ the HETDEX observing strategy, including realistic pointing pattern, observational magnitude constraints, and spectral sensitivity limits to generate a set of realistic observations which are then used with perfect and less than perfect knowledge scenarios to determine the cluster properties.

In all cases, we will attempt to characterize the observable–mass relation (or relations) to better understand the dominate sources of uncertainty when using HET-

DEX like observations. This will enable us to more fully understand and constrain the HMF which, in turns, allows us to make more accurate measurements of the cosmological parameters traced by galaxy clusters.

The second effort of this work, outlined in Section **??**, will use targeted spectroscopic observations of ten nearby clusters with the Mitchell Spectrograph (formerly known as VIRUS-P; Hill et al. 2008b), an integral field unit (IFU) in a square array of 246 4.24″ diameter optical fibers, to test some of the methods used in the first method. This will provide insight in how the observable–mass relation may be improved through followup observations of targeted clusters.

2. LITERATURE REVIEW: THE IMPORTANCE OF RESEARCH PART TWO- THIS IS DESIGNED TO TEST LONG TITLES IN THE TOC

2.1 INTRODUCTION

Our ability to perform precision cosmology with clusters of galaxies has reached a critical turning point. The widely accepted ΛCDM model of cosmology makes explicit predictions about the number and masses of galaxy clusters throughout the universe. However, connecting these predictions to a set of, sufficiently large in size, observed clusters remains a principal problem. Specifically, the largest threat to modern, precision, cluster cosmology is not the identification of large numbers of clusters (the total number of clusters known is only going up) but the accurate recovery of galaxy cluster mass (e.g., Sehgal et al. 2011; Planck Collaboration 2013; Bocquet et al. 2015).

As mass is not a direct observable, a lot of work is underway to characterize galaxy cluster masses with an observable feature of galaxy clusters. The goal is to constrain, as best possible, $P(X|M, z)$ the probability (P) that a galaxy cluster of given mass (M), located at redshift (z) determined using observable parameter (X). The observable parameter most commonly observed X-ray temperatures and luminosities (e.g., Mantz et al. 2010; Rykoff et al. 2014; Mantz et al. 2015), cosmic microwave background observations (e.g., Vanderlinde et al. 2010; Sehgal et al. 2011) using the Sunyaev-Zel'dovich effect (SZE; Sunyaev and Zeldovich 1972) or optical studies (e.g., Rozo et al. 2010, 2015) of richness (e.g., Abell 1958; Rykoff et al. 2012) or galaxy velocity dispersions (e.g., Ruel et al. 2014; Sifón et al. 2015b).

Massive surveys, both on going and planned, are revolutionizing cluster cosmology using a large range of wavelengths. The South Pole Telescope (SPT; Carlstrom

et al. 2011) and the Atacama Cosmology Telescope (ACT; Swetz et al. 2011) are discovering many clusters through the SZE. Optically, the on going The Dark Energy Survey (DES; The Dark Energy Survey Collaboration 2005) and planned Large Synoptic Survey Telescope (LSST; LSST Dark Energy Science Collaboration 2012) will identify many thousands of clusters to much lower masses than is possible with SZE measurements. However, regardless of the discovery method used, spectroscopic followup is needed to further constrain $P(X|M,z)$. But as the cluster dataset grows to many tens of thousands of clusters individual followup becomes increasingly impractical. Therefore, large spectroscopic surveys are needed to more fully constrain the observable–mass relation of clusters.

The Hobby Eberly Telescope Dark Energy eXperiment (HETDEX; Hill et al. 2008a) is a trailblazing effort to observe high-redshift large scale structures using cutting edge wide-field integral field unit (IFU) spectrographs. Designed to probe the evolution of the dark energy equation of state etched onto high redshift ($z > 2$) galaxies by the Baryon Acoustic Oscillations (Eisenstein et al., 2005) in the first moments of the universe, the survey will observe two fields for a total of 420 degree^2 from two fields (300 degree^2, Spring field and 120 degree^2, Fall field). Tuned to find Lyα emitting (LAE) galaxies at $1.9 < z < 3.5$, HETDEX expects to find 800,000 LAEs, and more than one million [O II] emitting galaxies at $z < 0.5$ masquerading as high-redshift galaxies (Acquaviva et al., 2014).

While a large portion of the $\sim 10^6$ interloping [O II] galaxies will be field (not associated with a bound structure) galaxies, the large area covered by HETDEX is expected to contain as many as 100 Virgo-sized ($M_{dyn} \sim 10^{15}$ M$_\odot$) clusters at $z < 0.5$ (citation?). The near-complete spectroscopic coverage allows an unprecedentedly detailed look at a very large number of clusters ranging from group scales to the very massive. In addition to the recovery of accurate dynamical masses, detailed

investigations of the of dynamical state of the clusters is possible.

Connecting the dynamical properties derived from spectroscopy to the properties inferred from other studies insures the greatest impact on future work. HETDEX overlaps with the Sloan Digital Sky Survey (SDSS; Blanton et al. 2001), SDSS stripe 82 (Annis et al., 2014), the Dark Energy Survey (DES; The Dark Energy Survey Collaboration 2005), and the upcoming DECam/IRAC Galaxy Environment Survey (DIRGES; PI: Papovich, C. Papovich et al. in preparation). SHELA and others? Would be good to have a whole list of different things and different wavelengths. While the potential dataset is very rich, two large issues remain.

It is unclear how a blind spectroscopic survey with an IFU will effect the recovery of galaxy cluster dynamical properties. Unlike many previous large cluster surveys (e.g., Milvang-Jensen et al. 2008; Robotham et al. 2011; Sifón et al. 2015b) which use multi-object spectrographs, the Visible Integral-Field Replicable Unit Spectrograph (VIRUS; Hill et al. 2012) used by HETDEX samples the sky unevenly which could excluded member galaxies which would otherwise be included. Secondly, it is not straightforward to use spectroscopic redshifts predominately from emission-line galaxies to interpret the kinematic and dynamical states of the clusters.

This work plans to address these concerns in the following ways. We use simulated observations which target individual galaxy clusters to investigate the recovery of parameters with such observations. Secondly, we create and evaluate a HETDEX like selection "function" of galaxies over a similarly large portion of the sky and use well adopted techniques to recover the dynamical properties, such as velocity dispersion and mass. Each observation strategy will further be constrained with "ideal" and "realistic" knowledge. Ideal knowledge assumes that we know which individual galaxy is assigned to which cluster. With realistic knowledge this is unknown and must be determined prior to the estimation of the cluster properties. Both of these

strategies will better allow future work to predict the number and types of galaxy clusters which should be observed with VIRUS during both the HETDEX survey portion and through targeted follow up observations.

We begin in Section 2.2 by giving an overview of what data is used, how it is created, and how we make our "observations." Details about the determination of cluster parameters, velocity dispersion, total mass, etc., are discussed in Section 2.3. Next, we present the results of our study in Section 2.4 and discuss their implications in Section 2.5. Finally we summarize our findings in Section 2.6.

Throughout this paper, we adopt the following cosmological model ($\Omega_\Lambda = 0.77$, $\Omega_M = 0.23$, $\sigma_8 = 0.83$ and $H_0 = 72$ km s^{-1}Mpc^{-1}), assume a Chabrier initial mass function (IMF; Chabrier 2003), and use AB magnitudes (Oke, 1974).

2.2 Data and Mock Observations

Blah blah intro stuff... Lorem ipsum dolor sit amet, consectetur adipisicing elit, sed do eiusmod tempor incididunt ut labore et dolore magna aliqua. Ut enim ad minim veniam, quis nostrud exercitation ullamco laboris nisi ut aliquip ex ea commodo consequat. Duis aute irure dolor in reprehenderit in voluptate velit esse cillum dolore eu fugiat nulla pariatur. Excepteur sint occaecat cupidatat non proident, sunt in culpa qui officia deserunt mollit anim id est laborum.

2.2.1 The "Buzzard" Catalogs

The "Buzzard" mock galaxy catalogs (R. Wechsler et al., private communication) cover 375.68 degree^2 between $60 < RA < 90$ and $-61 < DEC < -41$ and are derived from a combination of Sub-halo Abundance Matching (ShAM) and ADDSEDs (Adding Density Dependent Spectral Energy Distributions) tied to an in house n-body cosmological simulation. A brief description of the catalog creation is described as follows. The initial conditions are generated with a second-order Lagrangian per-

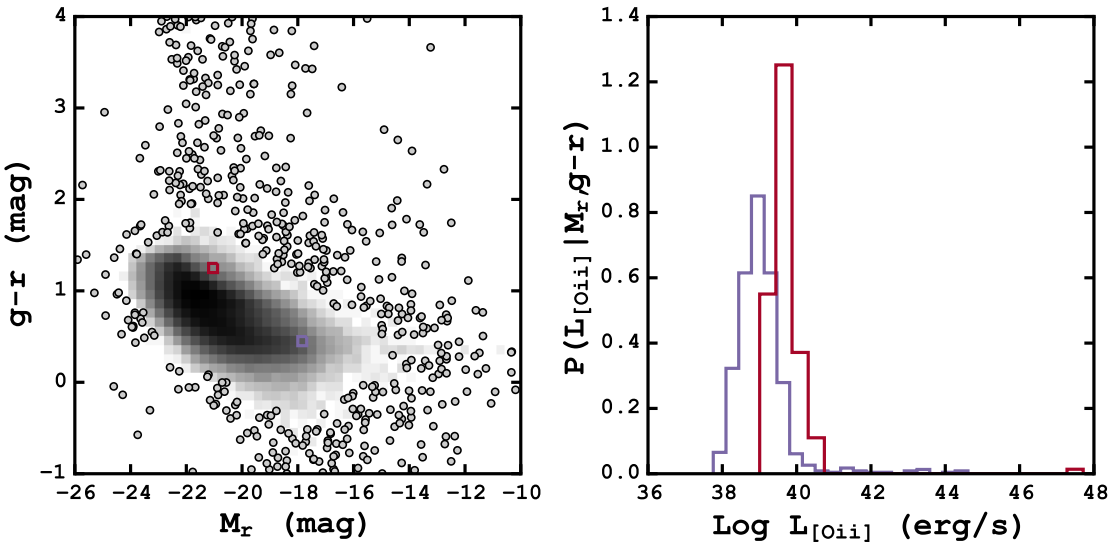

Figure 2.1: *Left*: CMD of 503113 $z < 0.2$ galaxies take from the SDSS DR12 where the shading scales with the density of points. The two boxes show regions containing potential catalog galaxies. *Right*: Probability histograms of the Log [O II] luminosity for the SDSS galaxies located in the two highlighted regions on the right. New [O II] luminosity (and subsequently fluxes) are assigned to catalog galaxies from slice sampling the probability histogram.

turbation theory using `2LPTic` (Crocce et al., 2006). Dark matter (DM) n-body simulations are run using `LGadget-2` (a version of `Gadget-2`; Springel 2005). The DM halos are identified using the `ROCKSTAR` halo finder (Behroozi et al., 2013) which also calculates halo masses and other various parameters.

Galaxy M_r luminosities are added to the velocity peaks using ShAM (Reddick et al., 2013), and ADDSEDs (Adding Density Dependent Spectral Energy Distributions) assign luminosities in the other bands. A M_r-density-SED relation is created using a SDSS training set, and for each mock galaxy the SED of a randomly selected training set galaxy which has a similar M_r and density is assigned. The result is a 398.49 sq. degree mock catalog occupying a $60 \leq RA \leq 90$ and $-40 \leq DEC \leq -61$ portion of the sky. It contains 238 million galaxies with r mag < 29 and $z \leq 8.7$.

The catalog information, used in this study, is broken into two large portions. The "truth" files contain the characteristics of each individual galaxies, such as right ascension (RA), declination (DEC), redshift (z), observed and rest-frame magnitudes, and many others. The "halo" files contain information for individual halos, to which many individual galaxies may belong. This includes five estimations of dynamical mass, RA, DEC, z, three dimensional velocity dispersion, and many others.

However, the catalogs do not include information on emission or absorption lines or estimations of whether the halo is relaxed or not. We supplement the catalogs with this information and describe the method in Section 2.2.2 and others.

We investigate the accuracy of the halo mass distribution by comparing the cumulative number density of halos above a mass (M_{200c}) threshold to the halo mass function (HMF) of Tinker et al. (2008). Shown in Figure **??** the HMF is calculated at central redshifts of 0, 0.2, and 0.4 using `HMFcalc` (Murray et al., 2013) and compared to galaxies in a redshift window of $\Delta z \pm 0.01$. We find a very good agreement between the expected HMF and the observed.

2.2.2 [O II] *Luminosity*

The Buzzard "truth" catalog does not provide [O II] luminosities so we must assign them empirically. We use 503113 galaxies from the SDSS Data Release 12 (Alam et al., 2015) from $z = 0.05 - 0.2$, which are selected with no redshift warning, and place each galaxy on a color-magnitude diagram (CMD) of M_r and $g - r$, see Figure 2.1.

To assign an [O II] luminosity to each galaxy in our catalog we place the catalog galaxies on the same CMD and select all SDSS galaxies in a small 2D (M_r, $g-r$) bin around the galaxy. We extract all of the SDSS galaxies inside that bin and create a histogram of their [O II] luminosities. Using a slice sampling technique (Neal, 1997) we assign the catalog galaxy an [O II] luminosity based on the distribution of SDSS galaxies extracted. For catalog galaxies which are placed on the CMD near no, or very few ($1 \leq n < 10$) galaxies we assign it zero [O II] luminosity or the mean luminosity, respectively.

The right panel of Figure 2.1 shows the CMD of all SDSS galaxies. Two potential catalog galaxies are also placed on the CMD ($M_r, g - r = -17.7,\ 0.49$ and $M_r, g - r = -21.4,\ 1.24$) and indicated by two colored boxes. The histograms show in the Figure's left panel shows the probability density histograms of the Log [O II] luminosity for the SDSS galaxies in the 2D bin. We sample the distribution and assign each catalog galaxy an [O II] luminosity which is then converted into a flux.

2.2.3 *Mock Observations*

Not sure this does a good enough job talking about the two different observations.

Tentatively slated to start in the spring of 2016, HETDEX will perform blind spectroscopy (R $\sim$ 750 in $3500 - 5500$ Å) over two fields along the celestial equator. The 300 degree^2, spring field and 120 degree^2, fall field will have no preselected targets.

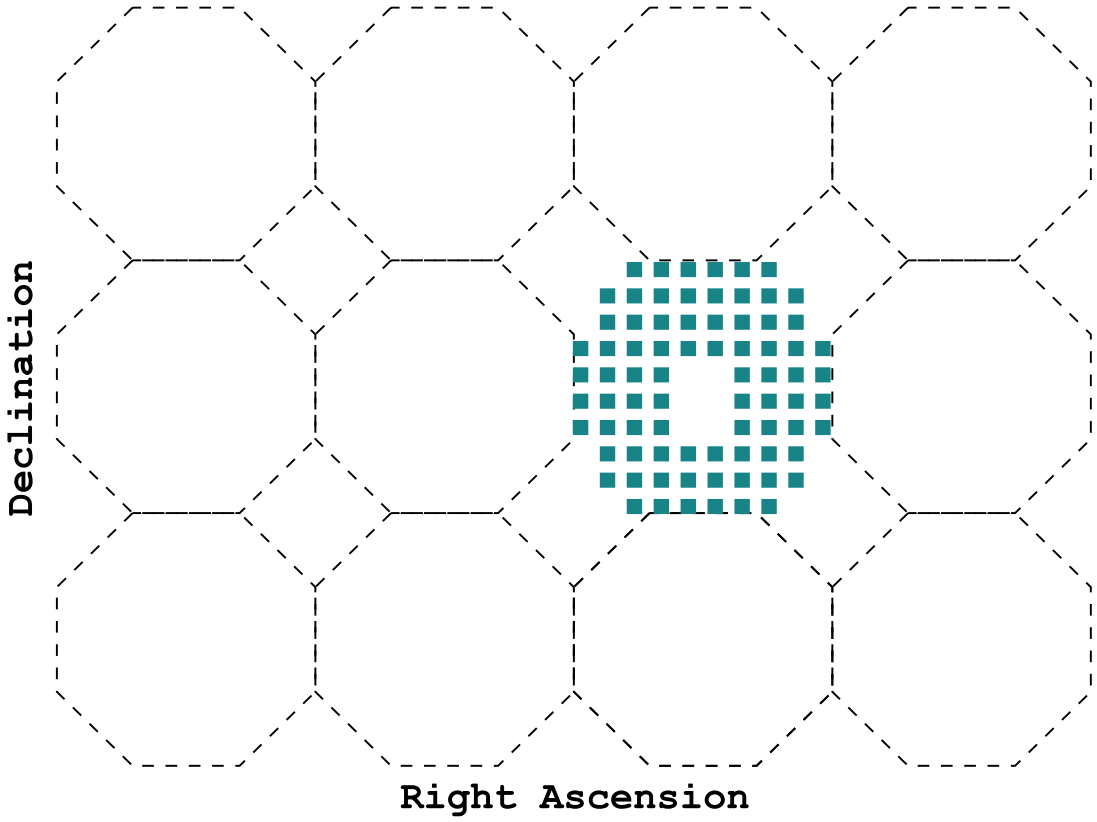

Figure 2.2: Representative observation tiling scheme for the HETDEX $16' \times 16'$ pointings. Each colored square is a single VIRUS IFU and the dashed octagons approximate the size of a single observation. See the text for more details.

Using VIRUS on the 10-m Hobby-Eberly Telescope (HET; Ramsey et al. 1998) the completed survey is expected to have an overall fill-factor of 1/4.5, meaning that the entire area could be covered with 4.5 dithers of the entire survey.

The spectral coverage allows for the detection of [O II] ($\lambda\lambda 3727 - 3729$ Å doublet) emitters to $z \sim 0.5$ and Ca H ($\lambda 3968.5$ Å) and K ($\lambda 3933.7$ Å) absorption features to $z \sim 0.4$. HETDEX is expected to detect sources with continuum brighter than 22 mag in g, and emission line strengths above 3.5×10^{-17} erg s^{-1} cm^{-2}. So we "observe" galaxies which meet either the emission line or magnitude requirements.

In this work we consider two separate observation cases. The first are targeted observations where we select each galaxy cluster and "observe" each galaxy within $8'$ of the center. The second is a survey case where observations which are blind to the positions of the clusters are conducted. In both cases, our "observations" consist of placing masks down onto the Buzzard "truth" catalogs and selecting all, $z < 0.5$ also meeting sensitivity limits, galaxies which lie underneath. Each mask is created to accurately reproduce the HETDEX IFU pattern, see Figure 2.2. The pattern consists of 78 IFUs, which are comprised of 448 optical fibers subtending a $50'' \times 50''$ region on the sky (Kelz et al., 2014). The inter-IFU spacing is also $50''$ spanning a total area of $16' \times 16'$ on the sky.

The individual IFUs have a fill-factor of 1/3, which will be completely filled with three dithers of the telescope at each pointing. This means that when selecting galaxies from the Buzzard catalog we assume an observation for all galaxies laying within a colored, IFU square in Figure 2.2. This should be updated with the fiber collisions. Galaxies which lie between the IFUs are missed, as well as the galaxies which lie between the pointings, as there is no overlap between one pointing and the next. To cover the 375.67 degree^2 field of the Buzzard catalog we require 5370 pointings where 0.015 degree^2 of each pointing is covered by an IFU. The total area of the sky covered by an IFU is 80.80 degree^2 which gives a filling factor of 1/4.65 slight decreased from the expected filling factor of 1/4.5.

2.3 Recovery of Parameters

In the following sections, we outline the methods we use to derive the dynamical properties of the galaxy clusters in our sample. This is not meant to be an exhaustive study of the different methods used to recover these parameters. The following is, in many cases, a subset of the available methods to derive any single parameter. The

specific choice of method may improve or diminish the accuracy of the recovered parameter, but the methods chosen were to facilitate comparison with observational studies.

2.3.1 Cluster Redshift

The accurate determination of the cluster redshift (z_c) is crucial to the reliability of all following measurements. An incorrect cluster redshift introduces errors into the measured line-of-sight velocity (LOSV) and corresponding dispersion, which, in turn, contributes to errors associated with dynamical mass and radius.

In simple terms, the cluster redshift is the mean of the redshifts of all galaxies associated with the cluster. However, because the standard mean can be quite sensitive to outliers or otherwise contaminated data, we require a more resistant statistic, and turn to the biweight location estimator (Beers et al., 1990) which provides improved performance.

2.3.2 Line-of-Sight Velocity Dispersion

We first calculate the line-of-sight velocity (LOSV) to each galaxy, where

$$LOSV = c\frac{z - z_c}{1 + z_c} \tag{2.1}$$

and c is the speed of light in km s^{-1}, z is the redshift of the individual galaxy, and z_c is the overall cluster redshift described in the previous section.

The line-of-sight velocity dispersion (LOSVD) is calculated using a method of maximum likelihood following Walker et al. (2006). We maximize the probability function

$$p(\{v_1, ..., v_N\}) = \prod_{i=1}^{N} \frac{1}{\sqrt{2\pi(\sigma_i^2 + \sigma_p^2)}} \exp\left[-\frac{1}{2}\frac{(v_i - \langle u \rangle)^2}{(\sigma_i^2 + \sigma_p^2)}\right] \tag{2.2}$$

where σ_p, $\langle\mu\rangle$, and σ_i is the LOSVD, the average radial velocity and the error on the individual LOSVs respectively. Using a Monte Carlo Markov Chain (MCMC) sampler (`emcee`); Foreman-Mackey et al. 2013), we draw twenty thousand samples from the posterior probability distribution. Simple priors, $\langle\mu\rangle$ lies between the maximum and minimum LOSV and $0 < \sigma_p$ check, are used. When the full distribution of LOSVDs are not used, the final LOSVD is quoted as the median value of the posterior probability distribution with 68% error bars defined as the 16th and 84th percentiles of the same distribution.

In principle, a single statistic such as the biweight scale estimator or the gapper estimator (both from Beers et al. 1990) with many bootstrap resamplings could be used to construct a distribution of σ_p. In simple tests where the values of both σ_p and $\langle\mu\rangle$ are known. The 68% error bars derived from the MCMC method give slightly better results with the true LOSVD value bracketed by the error bars in $\sim$ 68% of the cases versus $\sim$ 57% with bootstrapping and a single statistic. In addition, we prefer the maximum likelihood method for its straight forward treatment of the errors in the LOSV measurements.

2.3.3 Dynamical Mass

Recently, the relationship between the LOSVD and dynamical mass has been the focus of several studies (e.g., Evrard et al. 2008; Saro et al. 2013; Sifón et al. 2013; van der Burg et al. 2014), and a best fitting relationship for the mass enclosed by r_{200c} of the form

$$M_{200c} = \frac{10^{15}}{h(z)} \left(\frac{\sigma_{1D}}{A_{1D}} \right)^{1/\alpha} \mathrm{M}_\odot \tag{2.3}$$

with $A_{1D} = 1177 \pm 4.2$ km s^{-1} (Munari et al. 2013; referred to as σ_{15} in Evrard et al. 2008 and other works), $\alpha = 1/3$, $h(z) = H(z)/100$, and σ_{1D} is the LOSVD of the velocity tracers (dark matter particles, subhalos or galaxies).

A growing body of work suggests that there is a significant difference in the observed LOSVD depending on the velocity tracers used. Specifically, while there is little difference between using galaxies and their host DM subhalos, there is a significant over estimation of the LOSVD when using galaxies/subhalos compared to DM particles (Munari et al., 2013). We follow other works (e.g., Kirk et al. 2015; Sifón et al. 2015a) using the scaling relation, given in Equation 2.3 from Munari et al. (2013) to facilitate comparisons with other observational studies.

2.3.4 Dynamical Mass Corrections

In this section we use two methods to predict the mass of a cluster based on other observables. Often the cluster mass is estimated based on a single observable, X-ray temperature, velocity dispersion, richness and others. Here we combine many observables to attempt to correct the mass inferred solely from the velocity dispersion. The first method is traditional probability based where we marginalize over a series of observables to find the most probable mass. The second is based on a machine learning (ML) algorithm which attempts to "learn" the relationship between the observables and the desired output, the mass. Both of these methods are examples of supervised learning algorithms where the relationship between the observable (known) parameters and the target parameter (the mass) are both known.

As with any predictive analysis it is important to test the model on data that the model has not seen before. In this section we take all of the observed clusters, our full sample, split them, and generate a training and testing set. The data is randomly split 70% training and 30% testing. We follow the ML convention and refer to the individual clusters in each set as a "sample", and the parameters associated with the cluster (z, LOSVD, mass, etc.) as "features".

2.3.4.1 Probability Based

We begin with the training sample. After selecting the desired features $\vec{x} = \{\sigma, z, ...\}$ we make the joint probability between the true cluster mass (M) and $\vec{x}$. Because $\vec{x}$ can be multidimensional, we rely on the corner plot to visualize the relationship between all of the training features. Figure 2.3 shows all of the one (marginalized probability) and two (joint probability) dimensional projections of the posterior probability distributions of the features of the training data.

The conditional probability of the mass $P(M|\vec{x} = \{x_1, x_2, ...\})$ is determined by taking a slice through the joint probability distributions in bins centered on the desired value. The slices show by the colored bars in Figure 2.3 are centered on $\sigma =$ 500 km s^{-1}and $z = 0.17$. The distribution of mass contained in the three dimensional bin given by the intersection of these slices is $P(M|\vec{x} = \{\sigma = 500\text{km s}^{-1}, z = 0.17\})$.

For the clusters making up the *test* sample the mass is unknown (it is what we are trying to predict) but the other features are known. To determine the mass probability distribution of a test cluster, $P(M)$ we combine the conditional probability distribution, $P(M|\vec{x})$, created previously with the probability distribution of σ through Equation 2.4.

$$P(M) = \int P(M|\vec{x})P(\sigma)d\sigma \tag{2.4}$$

The expected mass is determined by integrating the mass probability, $P(M)$ over all mass. This becomes our "predicted" mass, $\langle M \rangle$.

$$\langle M \rangle = \int M' P(M')dM' \tag{2.5}$$

The confidence interval associated with this prediction can be estimated two ways.

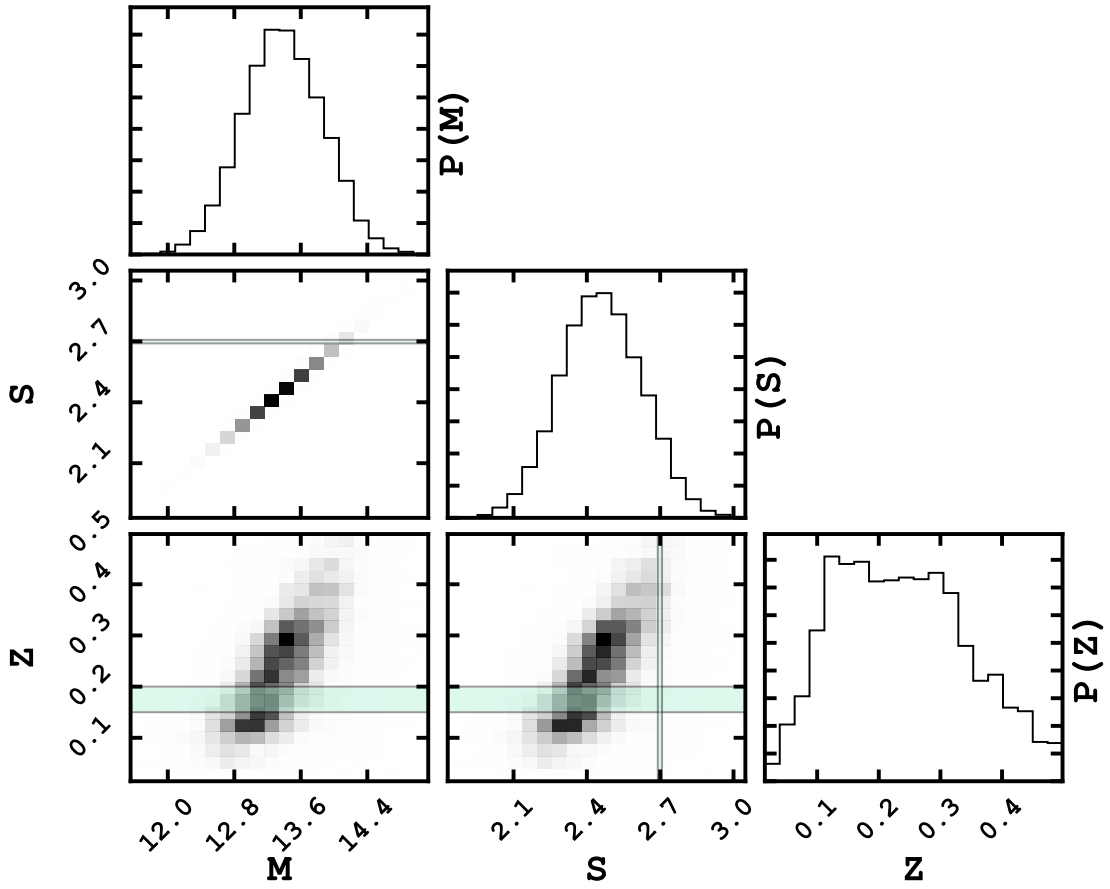

Figure 2.3: Corner plot of the *training* data with features σ and z. The corner plots shows all of the one and two dimensional posterior probability distributions used to determine the correct cluster mass. The colored rectangles show the slices needed to create a conditional probability distribution of the mass, $P(M|\vec{x})$. See text for a complete description.

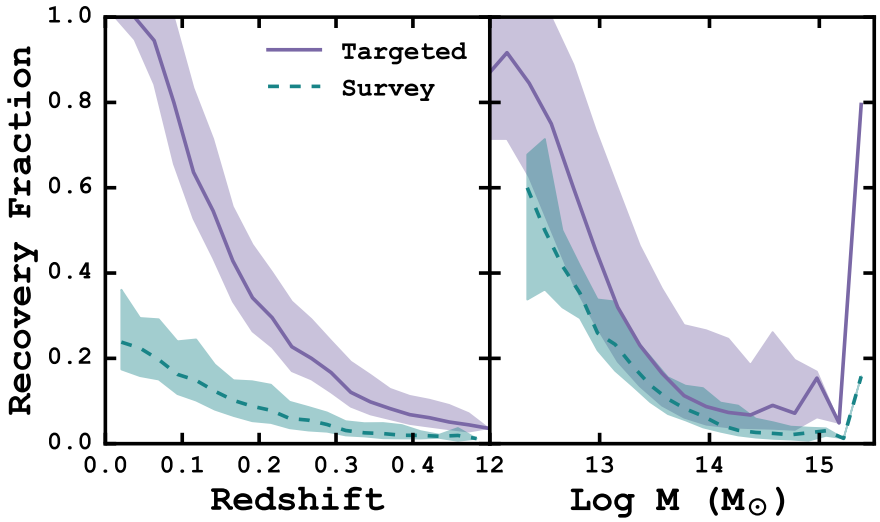

Figure 2.4: Recovery fractions (N_{obs}/N_{True}) of cluster member galaxies as a function of redshift and mass for the targeted and survey observing strategies. The solide lines are the median values and the shaded regions represent the 68% scatter. The significant decline in galaxies observed with the survey strategy is due to gaps in the VIRUS IFU.

First, by calculating the variance about the expected mass through

$$V = \int (M' - \langle M \rangle)^2 P(M') dM' \tag{2.6}$$

or by drawing many samples from $P(M)$ and calculating the values at the 16th and 84th percentile. In practice we find that both methods produce similar results for a large number of trials. Therefore, we quote predicted masses as the most probable mass given by Equation 2.5 and associated 68% error estimated through Equation 2.6.

2.3.4.2 Machine Learning Based

The estimation in this section relies on a ML technique known as an ensemble method, where many estimators are created by a single learning method with the goal of improved generalization and robustness compared to a single estimation.

Ensemble methods come in two general flavors. Averaging methods average (hence the name) the estimators to produce a single prediction. Boosting estimators build estimates sequentially by attempting to address poor performing estimators in each previous step, hence "boosting" the predictive power.

Here we use an averaging ensemble learning method known as a forest of randomized decision trees often shorten to just random forest (RF). Decision trees can be visualized a flow chart where forks are the branches of the tree. The path along the tree is decided by the values of the feature at each branch. RF estimators use a random subset of the training set at each fork to decide which path should be followed. The final prediction is then the average of all the trees. We use RF regression methods as implemented in `Scikit-Learn` (Pedregosa et al., 2012).

Any uncertainties quoted by this method are prediction intervals not confidence intervals. A prediction interval is an estimate of the interval encompassing future observations, with a certain probability. And, unlike confidence intervals, which describe certainties on the different moments of a population, a prediction interval is unique to each prediction. In many regresson analyses, such as linear fitting, the prediction intervals are based on underlying assumptions of normally distributed residuals. However, RF estimators do not have any such assumptions and require special treatment.

The prediction intervals here are based on the general method of quantile regression forests (Meinshausen, 2006). The general idea is that all response variables are recorded, not just the mean. Then the prediction can be returned as the full conditional probability distribution of all responses, which allows us to generate the prediction intervals. The 68% prediction interval is determined by calculating the 16th and 84th percentile of the full conditional probability distribution. I am going to change this to just the std of the distribution. I need the errorbars to be sysmetric

to make the fitting routine easy later on.

2.4 RESULTS

Here we explore the cluster member recovery rate and mass estimates for the two observing strategies. We discuss the accuracy of dynamical mass derived from both the scaling relation (see Equation 2.3) and through the probability and ML methods.

2.4.1 Recovery of Cluster Members

As discussed in Section 2.2.3 the observational constraints place limits on the total number fo clusters member galaxies expected to be recovered. Knowing these limits will provide important information for potential future follow up or targeted observations.

Figure 2.4 shows the recovery fraction of member galaxies, the number of observed galaxies divided by the number of actual galaxies (N_{obs}/N_{True}), as function of both redshift and cluster mass. It is important to note that if few than five member galaxies are observed the cluster is not considered detected, and is excluded from this figure. As expected, the targeted observing strategy where the individual clusters are targeted through several dithers to ensure near complete coverage, performs significantly better than the survey observing strategy across all redshifts and cluster masses.

For the clusters recovered as a function of redshift, there are two effects at work. The decrease in recovery fraction with increasing redshift is a magnitude effect. If, instead of being limited to 22 mag in $g$apparent, the observations where limited by absolute magnitude, the sharp downward trend disappears. The second key feature is the strong decline in clusters recovered from survey observations. This is due to gaps in the VIRUS IFU. The median recovery fraction in survey observations is almost exactly 4.5 times less than the targeted median recovery fraction. As the total filling

factor of the survey increases the two lines will converge.

The recovery rate as a function of cluster mass, right panel of Figure 2.4, shows that of the the low mass clusters we detect ($N_{obs} > 5$), observe the majority of the galaxies. This also shows a rapid decrease in the detection fraction, which can again be explained by considering absolute magnitudes instead of apparent magnitudes. Just as before, if the survey was limited by absolute magnitude, we find a much more consistent detection fraction.

2.4.2 Mass estimates

In this section we discuss the how accurately we are able to reproduce the true cluster mass from a set of observations. We report on two methods the probability based approach (Section 2.3.4.1) and the ML based method (Section 2.3.4.2). For each method we consider both targeted and HETDEX-like observing strategies.

In both figures, we include the cluster masses recovered through the power law scaling relation given in Equation 2.3 for both the targeted and survey observations. It should serve as baseline to compare the probability based and ML cluster mass recovery methods. And, while there are many possible metrics to evaluate performance, we compute two: the median absolute error (MAE) and the root mean squared error (RMSE). Both metrics evaluate how closely the ensemble of predicted cluster masses are to the true cluster masses, and in both cases lower numbers are better.

Just because a predicted cluster mass may not exactly match the true value does not mean it is a bad prediction. In addition to the MAE and RMSE, we also report the fraction of predictions where the the true cluster mass is contained within the 68% confidence or prediction intervals (see Sections 2.3.4.1 and 2.3.4.2).

The cluster masses predicted by Equation 2.3 gives the following results. The

MAE is 0.263 dex and for both the targeted and survey observations. The RMSE is 0.396 dex and 0.394 dex for the targeted and survey observations respectively. This scatter in recovered masses can be attributed to both physical and numerical effects. As the cluster mass increases, clusters become more virialized and contain many individual galaxies. The presence of any in-falling matter onto lower mass clusters can introduce a significant amount of substructure, which can increase the observed LOSVD increasing the predicted mass. Also, as the number of cluster galaxies decreases the LOSVD PDF is poorly sampled leading to poorly recovered cluster masses due to numerical effects. The masses presented here are recovered using the best possible conditions, where we have perfect knowledge of the cluster membership. In reality, the mass recovery levels presented in this section represent an upper bound (the best) on the accuracy achievable through this method. Ntampaka et al. (2015) does have a discussion about how well they do with contaminated galaxy catalogs. We could do something similar and have a similar discussion, but I'm not sure it is worth it. Should be simple enough to do with the targeted catalog, but with the HETDEX catalog it would be pretty bad IMO. We should also talk about how often the true mass lies within the error bars. Many of them are going to be with the 68% range, but we can drop the error estimates to 0.5σ if that actually means anything

The MAE and RMSE associated with the ensemble of predictions are summarized in Table 2.1. As expected, we find that both the probability based and ML based methods out perform the standard power law based methods for both the targeted and survey observations. We also find that the ML based method produces lower ensemble error for both the observation strategies when compared to the probability based method, although the MAE and RMSE are reduced by only ~ 0.01 dex. here is where we would talk about cross validation on the errors.

Table 2.1: Summary of the errors associated with the Targeted and Survey observation strategies, as an ensemble of predictions. See the text for discussion about the MAE and RMSE. Overlap is the percentage of clusters where the true cluster mass is bracketed by the prediction intervals of the predicted mass. See Sections 2.3.4.1 and 2.3.4.2 for a discussion on prediction intervals.

		Targeted			Survey		
	Input Features	MAE (dex)	RMSE (dex)	Overlap (%)	MAE (dex)	RMSE (dex)	Overlap (%)
Prob Based	Power Law	0.263	0.396	—	0.263	0.393	—
	σ	0.220	0.335	—	0.222	0.329	—
	σ, z	0.189	0.286	—	0.194	0.278	—
	σ, z, N_{gal}	0.129	0.207	—	0.140	0.222	—
ML Based	Power Law	0.263	0.396	—	0.263	0.393	—
	σ	0.246	0.361	—	0.238	0.344	—
	σ, z	0.193	0.285	—	0.171	0.260	—
	σ, z, N_{gal}	0.117	0.193	—	0.093	0.179	—

In both Figures 2.5 and 2.6, we show the predicted versus true cluster masses for each of the two observing strategies. In each panel the solid black line is the 1:1 relationship, the solid colored line is the median recovered mass for the targeted observing, and the colored, dashed line is the median recovered mass for the HETDEX-like observations. The shaded regions are the 68% scatter around the median values (the 16% and 84% quartiles). The lower panels show the fractional cluster mass error:

$$\epsilon = (M_{pred} - M)/M \tag{2.7}$$

where M_{pred} is the predicted cluster mass and M is the true cluster mass.

In both figures we successively add additional information to further contrain the true cluster masses which subsequently reduces the error associated with the ensemble of predictions (see Table 2.1). The power law derived masses, using the single (not including the cosmological parameters) free parameter, σ (the LOSVD),

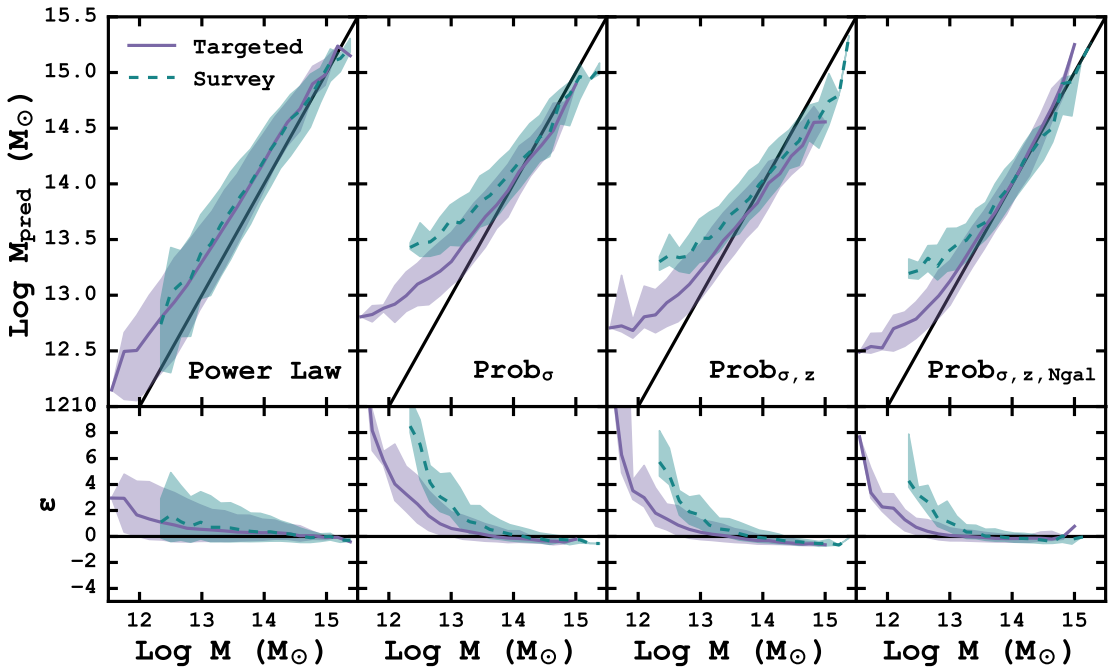

Figure 2.5: Mass predictions for the power law scaling relation (Equation 2.3) and the probability based technique with different input features as a function of true cluster mass. The bottom row of panels shows the fractional error (Equation 2.7) also as a function of true cluster mass. The solid black line shows the 1:1 relation. The solid, colored line is the median predicted mass for the targeted observing, and the colored, dashed line is the median recovered mass for the HETDEX-like observations. The shaded regions represent the 68% scatter around the median values.

over estimates the predicted cluster mass at all masses. Both the probability and ML methods over predict the mass of low mass clusters and under predict the mass of the higher mass clusters. When the redshift information is also added, the amount of this over and under prediction is lessened but the cross over point, remains roughly consistent at $\sim 10^{14}$ M$_\odot$. Additionally, the number of galaxies observed, N_{gal}, further reduces the MAE and RMSE on the predictions but also lowers the cross over point to $\sim 10^{13.5}$ M$_\odot$.

Need to talk about the cluster rotations to fill out the survey data. Otherwise

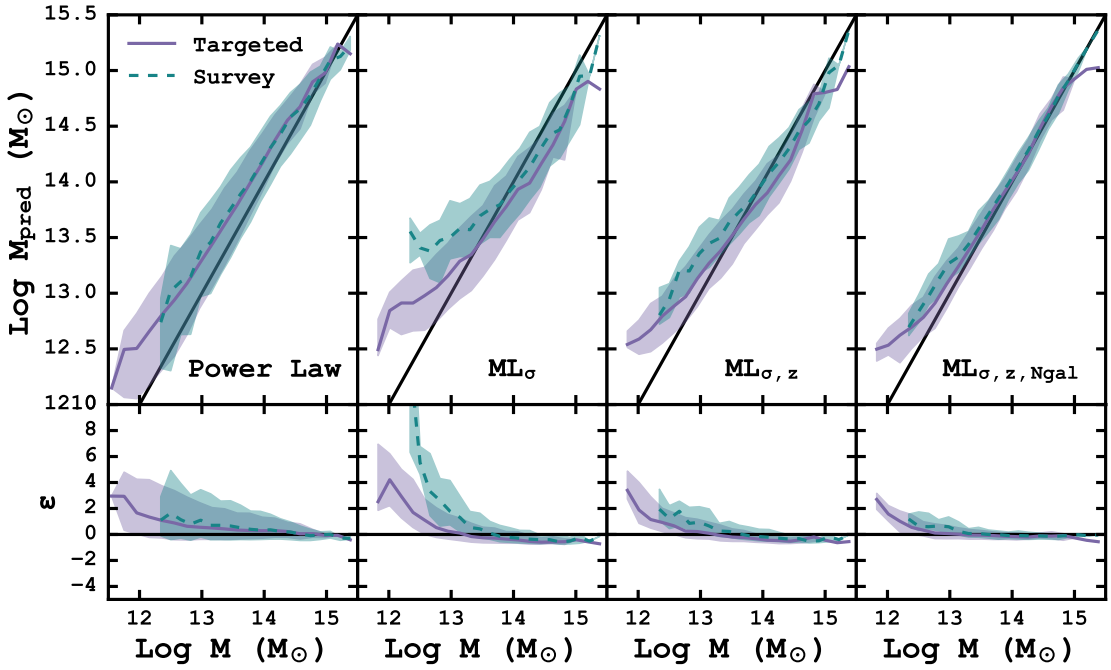

Figure 2.6: Mass predictions for the power law scaling relation (Equation 2.3) and the ML based technique with different input features as a function of true cluster mass. The bottom row of panels shows the fractional error (Equation 2.7) also as a function of true cluster mass. The solid black line shows the 1:1 relation. The solid, colored line is the median predicted mass for the targeted observing, and the colored, dashed line is the median recovered mass for the HETDEX-like observations. The shaded regions represent the 68% scatter around the median values.

there aren't that many clusters detected.

2.5 HETDEX as a Galaxy Cluster Survey

2.5.1 Extendability to Other Surveys

Large-scale optical surveys (e.g., DES and LSST) expect to detect hundreds of thousands of galaxy clusters at $z < 1$. Because they are photometric, a major challenge for these surveys is relating a cluster observable to the total dark-matter mass. One promising mass estimator is the optical richness (e.g., Abell 1958). Specifically,

here, we use λ, the weighted number of galaxies within a scale aperture (e.g., Rozo et al. 2011) as calculated by the redMapper algorithm (Rykoff et al., 2012). Previous works (e.g., Rozo et al. 2010) show that the richness correlates strongly with cluster mass on the average, but the absolute mass scale of the optical richness mass estimator and the scatter in cluster mass at fixed optical richness are imprecisely known (Rykoff et al., 2012). These systematics remain the major source of uncertainty in deriving cosmological constraints from cluster abundances and must be measured using independent methods to realize the full potential of these surveys.

We leverage the large spectroscopic dataset of HETDEX to estimate its ability to constrain the scatter and absolute scale of the richness-mass relationship. We begin by cross matching both the targeted and survey observations with a redMapper catalog. The redMapper catalog is limited to $\lambda >= 20$, or at least twenty object assigned to each cluster. With the targeted and survey observations, we observe 138 and 58 clusters respectively.

Figure 2.7 shows the optical richness, λ, versus the predicted cluster mass. The cluster masses are the $ML_{\sigma,z,N_{gal}}$ based and correspond to the correct observation strategy. The error bars represent the 1σ prediction intervals for each cluster mass. The solid and dashed lines are fits to the targeted and survey datasets. For comparison, the richness-mass relations from Rykoff et al. (2012) (their equation B5) is shown as a dash-dotted line.

To generate the best fitting lines we follow the general procedure of Hogg et al. (2010), by defining an objective function and then minimizing the loss. Our loss function is

$$\ln L = \frac{-1}{2}\left(\sum_{i=1}^{N}\frac{[y_i - mx_i - b]^2}{\sigma_{yi}} + \sum_{i=1}^{N}\frac{[y_i - mx_i - b]^2}{\sigma_{xi}}\right) \tag{2.8}$$

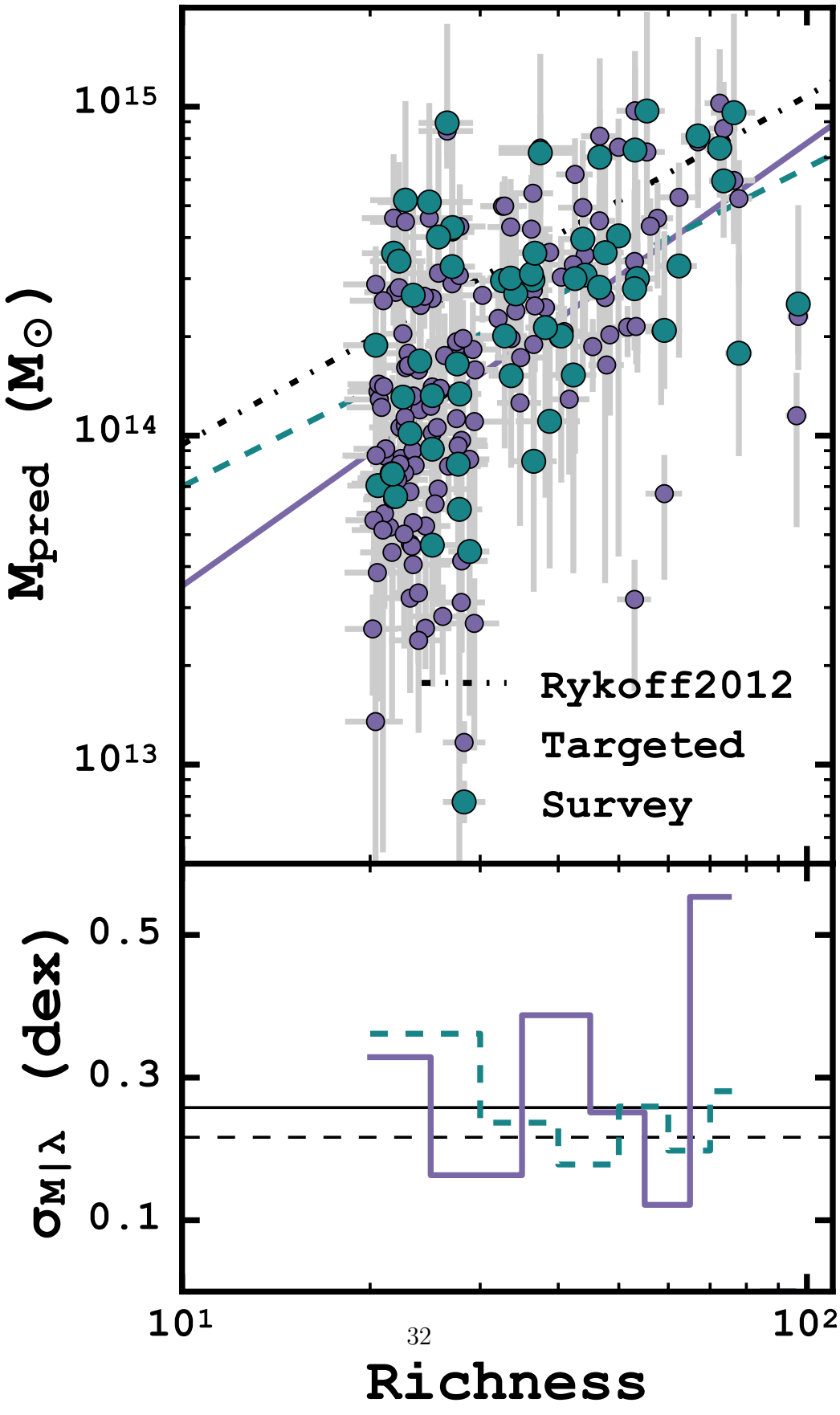
10^{15}
10^{14}
10^{13}
M_{pred} ($M_\odot$)
Rykoff2012
Targeted
Survey
0.5
0.3
0.1
$\sigma_{M|\lambda}$ (dex)
10^1
10^2
Richness

where we have taken into account the uncertainties in both the richness and predicted cluster mass. We again rely on MCMC samples to sample the posterior probability distribution. The best fitting slope and intercept are quoted as the median value of the posterior probability distribution with 68% error bars defined as the 16th and 84th percentiles of the same distribution.

Following the notation of Rykoff et al. (2012) we find a best-fitting relation for the targeted observations as

$$ln\left(\frac{M_{200c}}{h_{70}^{-1}10^{14}\mathrm{M}_{\odot}}\right) = 1 \pm 0.13 + 1.34 \pm 0.17 ln\left(\frac{\lambda}{60}\right)$$

and the survey observations as

$$ln\left(\frac{M_{200c}}{h_{70}^{-1}10^{14}\mathrm{M}_{\odot}}\right) = 1.02 \pm 0.13 + 0.96 \pm 0.22 ln\left(\frac{\lambda}{60}\right)$$

The bottom panel of Figure 2.7 shows the scatter in cluster masses at fixed richness, $\sigma_{M|\lambda}$. The solid and dashed lines represent the targeted and survey observations respectively, and have been offset from one another for clarity. The cluster masses are binned in increasing ten richness intervals ($20-30$, $30-40$, etc.). The two horizontal lines show the mean scatter of 0.26 dex for the targeted observations and 0.21 dex for the survey observations. While not shown in the figure, we find a mean scatter of 0.27 dex if we replace M_{pred} with the true cluster mass for the clusters identified with targeted observations.

We expect the targeted observations to have more scatter because the survey observations are

Much like the MAE and RMSE associated with the cluster mass recovery, comparing the individual $\sigma_{M|\lambda}$ values directly is incorrect. When comparing only the

clusters with observations in both the targeted and survey stratigies we

2.5.2 Potential Improvements

The potential improvements are really three fold. We know that the observing won't cover all of the sky. So we can simply tile more and try to get more clusters. We can observe deeper. I'm not sure the current exposure times (they are in an email that I sent to casey) but if we can extend them, then we can get further down the IMF and try to build up some of the clusters that are really more like groups than anything else. The last thing we can do is to attempt to build better models to make better predictions on the masses. That might be something like the study that Acquaviva (2016) did with the stellar metallicities. Or we'll need something else that I haven't thought of just yet. The other idea is to come up with some sort of cheat sheet for HETDEX. Basically, a if you detect such and such type of galaxy in the survey model then you should go back and try to follow it up with targeted observations. It might be good to talk about the recovery fraction between the two surveys above. Like... if there are 30 cluster members then we should detect the cluster in both surveys.

Lorem ipsum dolor sit amet, consectetur adipisicing elit, sed do eiusmod tempor incididunt ut labore et dolore magna aliqua. Ut enim ad minim veniam, quis nostrud exercitation ullamco laboris nisi ut aliquip ex ea commodo consequat. Duis aute irure dolor in reprehenderit in voluptate velit esse cillum dolore eu fugiat nulla pariatur. Excepteur sint occaecat cupidatat non proident, sunt in culpa qui officia deserunt mollit anim id est laborum.

2.6 SUMMARY

Lorem ipsum dolor sit amet, consectetur adipisicing elit, sed do eiusmod tempor incididunt ut labore et dolore magna aliqua. Ut enim ad minim veniam, quis nostrud

exercitation ullamco laboris nisi ut aliquip ex ea commodo consequat. Duis aute irure dolor in reprehenderit in voluptate velit esse cillum dolore eu fugiat nulla pariatur. Excepteur sint occaecat cupidatat non proident, sunt in culpa qui officia deserunt mollit anim id est laborum.

Our main conclusions are the following:

1. Lorem ipsum dolor sit amet, consectetur adipisicing elit, sed do eiusmod tempor incididunt ut labore et dolore magna aliqua. Ut enim ad minim veniam, quis nostrud exercitation ullamco laboris nisi ut aliquip ex ea commodo consequat. Duis aute irure dolor in reprehenderit in voluptate velit esse cillum dolore eu fugiat nulla pariatur. Excepteur sint occaecat cupidatat non proident, sunt in culpa qui officia deserunt mollit anim id est laborum.

2. Lorem ipsum dolor sit amet, consectetur adipisicing elit, sed do eiusmod tempor incididunt ut labore et dolore magna aliqua. Ut enim ad minim veniam, quis nostrud exercitation ullamco laboris nisi ut aliquip ex ea commodo consequat. Duis aute irure dolor in reprehenderit in voluptate velit esse cillum dolore eu fugiat nulla pariatur. Excepteur sint occaecat cupidatat non proident, sunt in culpa qui officia deserunt mollit anim id est laborum.

3. Lorem ipsum dolor sit amet, consectetur adipisicing elit, sed do eiusmod tempor incididunt ut labore et dolore magna aliqua. Ut enim ad minim veniam, quis nostrud exercitation ullamco laboris nisi ut aliquip ex ea commodo consequat. Duis aute irure dolor in reprehenderit in voluptate velit esse cillum dolore eu fugiat nulla pariatur. Excepteur sint occaecat cupidatat non proident, sunt in culpa qui officia deserunt mollit anim id est laborum.

It is the author's hope that this work may be useful to others when conducting their own research. Because this work relies heavily on (often) complex data analysis,

and in order to promote transparency, we provide all of the code used to conduct this study at https://github.com/boada/desCluster. Regrettably, large file size prevents including the source data with the analysis routines. The authors are happy to provide them, if requested.

3. LAST CHAPTER: THE IMPORTANCE OF RESEARCH

Text goes here **?**.

3.1 New Section

Figure 3.1: TAMU figure

3.2 Another Section

Text between the figures. Text between the figures. Text between the figures. Text between the figures. Text between the figures. Text between the figures. Text

between the figures. Text between the figures. Text between the figures. Text between the figures. Text between the figures. Text between the figures. Text between the figures.

3.2.1 Subsection

3.2.2 Subsection

A table example is going to follow.

Table 3.1: This is a table template

Product	1	2	3	4	5
Price	124.-	136.-	85.-	156.-	23.-
Guarantee [years]	1	2	-	3	1
Rating	89%	84%	51%		45%
Recommended	yes	yes	no	no	no

3.2.2.1 This is a subsubsection

3.3 Another Section

REFERENCES

George O. Abell. The Distribution of Rich Clusters of Galaxies. *ApJS*, 3:211, may 1958. ISSN 0067-0049. doi: 10.1086/190036. URL http://adsabs.harvard.edu/abs/1958ApJS....3..211A.

Viviana Acquaviva. How to measure metallicity from five-band photometry with supervised machine learning algorithms. *MNRAS*, 456(2):1618–1626, feb 2016. ISSN 0035-8711. doi: 10.1093/mnras/stv2703. URL http://adsabs.harvard.edu/abs/2015arXiv151008076A http://arxiv.org/abs/1510.08076 http://mnras.oxfordjournals.org/lookup/doi/10.109

Viviana Acquaviva, Eric Gawiser, Andrew S. Leung, and Mario R. Martin. Low/High Redshift Classification of Emission Line Galaxies in the HETDEX survey. *Proc. IAU*, 10(S306):365–368, may 2014. ISSN 1743-9213. doi: 10.1017/S1743921314013805. URL http://adsabs.harvard.edu/abs/2014arXiv1411.2651A http://www.journals.cambridge.org/abstract_S1743921314013805.

Shadab Alam, Franco D. Albareti, Carlos Allende Prieto, F. Anders, Scott F. Anderson, Timothy Anderton, Brett H. Andrews, Eric Armengaud, Éric Aubourg, Stephen Bailey, Sarbani Basu, Julian E. Bautista, Rachael L. Beaton, Timothy C. Beers, Chad F. Bender, Andreas A. Berlind, Florian Beutler, Vaishali Bhardwaj, Jonathan C. Bird, Dmitry Bizyaev, Cullen H. Blake, Michael R. Blanton, Michael Blomqvist, John J. Bochanski, Adam S. Bolton, Jo Bovy, A. Shelden Bradley, W. N. Brandt, D. E. Brauer, J. Brinkmann, Peter J. Brown, Joel R. Brownstein, Angela Burden, Etienne Burtin, Nicolás G. Busca, Zheng Cai, Diego Capozzi, Aurelio Carnero Rosell, Michael A. Carr, Ricardo Carrera,

K. C. Chambers, William James Chaplin, Yen-Chi Chen, Cristina Chiappini, S. Drew Chojnowski, Chia-Hsun Chuang, Nicolas Clerc, Johan Comparat, Kevin Covey, Rupert A. C. Croft, Antonio J. Cuesta, Katia Cunha, Luiz N. da Costa, Nicola Da Rio, James R. A. Davenport, Kyle S. Dawson, Nathan De Lee, Timothée Delubac, Rohit Deshpande, Saurav Dhital, Letícia Dutra-Ferreira, Tom Dwelly, Anne Ealet, Garrett L. Ebelke, Edward M. Edmondson, Daniel J. Eisenstein, Tristan Ellsworth, Yvonne Elsworth, Courtney R. Epstein, Michael Eracleous, Stephanie Escoffier, Massimiliano Esposito, Michael L. Evans, Xiaohui Fan, Emma Fernández-Alvar, Diane Feuillet, Nurten Filiz Ak, Hayley Finley, Alexis Finoguenov, Kevin Flaherty, Scott W. Fleming, Andreu Font-Ribera, Jonathan Foster, Peter M. Frinchaboy, J. G. Galbraith-Frew, Rafael A. García, D. A. García-Hernández, Ana E. García Pérez, Patrick Gaulme, Jian Ge, R. Génova-Santos, A. Georgakakis, Luan Ghezzi, Bruce A. Gillespie, Léo Girardi, Daniel Goddard, Satya Gontcho A Gontcho, Jonay I. González Hernández, Eva K. Grebel, Paul J. Green, Jan Niklas Grieb, Nolan Grieves, James E. Gunn, Hong Guo, Paul Harding, Sten Hasselquist, Suzanne L. Hawley, Michael Hayden, Fred R. Hearty, Saskia Hekker, Shirley Ho, David W. Hogg, Kelly Holley-Bockelmann, Jon A. Holtzman, Klaus Honscheid, Daniel Huber, Joseph Huehnerhoff, Inese I. Ivans, Linhua Jiang, Jennifer A. Johnson, Karen Kinemuchi, David Kirkby, Francisco Kitaura, Mark A. Klaene, Gillian R. Knapp, Jean-Paul Kneib, Xavier P Koenig, Charles R. Lam, Ting-Wen Lan, Dustin Lang, Pierre Laurent, Jean-Marc Le Goff, Alexie Leauthaud, Khee-Gan Lee, Young Sun Lee, Timothy C. Licquia, Jian Liu, Daniel C. Long, Martín López-Corredoira, Diego Lorenzo-Oliveira, Sara Lucatello, Britt Lundgren, Robert H. Lupton, Claude E. Mack III, Suvrath Mahadevan, Marcio A. G. Maia, Steven R. Majewski, Elena Malanushenko, Viktor Malanushenko, A. Manchado, Marc Manera, Qingqing

Mao, Claudia Maraston, Robert C. Marchwinski, Daniel Margala, Sarah L. Martell, Marie Martig, Karen L. Masters, Savita Mathur, Cameron K. McBride, Peregrine M. McGehee, Ian D. McGreer, Richard G. McMahon, Brice Ménard, Marie-Luise Menzel, Andrea Merloni, Szabolcs Mészáros, Adam A. Miller, Jordi Miralda-Escudé, Hironao Miyatake, Antonio D. Montero-Dorta, Surhud More, Eric Morganson, Xan Morice-Atkinson, Heather L. Morrison, Benoit Mosser, Demitri Muna, Adam D. Myers, Kirpal Nandra, Jeffrey A. Newman, Mark Neyrinck, Duy Cuong Nguyen, Robert C. Nichol, David L. Nidever, Pasquier Noterdaeme, Sebastián E. Nuza, Julia E. OConnell, Robert W. OConnell, Ross OConnell, Ricardo L. C. Ogando, Matthew D. Olmstead, Audrey E. Oravetz, Daniel J. Oravetz, Keisuke Osumi, Russell Owen, Deborah L. Padgett, Nikhil Padmanabhan, Martin Paegert, Nathalie Palanque-Delabrouille, Kaike Pan, John K. Parejko, Isabelle Pâris, Changbom Park, Petchara Pattarakijwanich, M. Pellejero-Ibanez, Joshua Pepper, Will J. Percival, Ismael Pérez-Fournon, Ignasi Perez-Ra'fols, Patrick Petitjean, Matthew M. Pieri, Marc H. Pinsonneault, Gustavo F. Porto de Mello, Francisco Prada, Abhishek Prakash, Adrian M. Price-Whelan, Pavlos Protopapas, M. Jordan Raddick, Mubdi Rahman, Beth A. Reid, James Rich, Hans-Walter Rix, Annie C. Robin, Constance M. Rockosi, Thaíse S. Rodrigues, Sergio Rodríguez-Torres, Natalie A. Roe, Ashley J. Ross, Nicholas P. Ross, Graziano Rossi, John J. Ruan, J. A. Rubiño-Martín, Eli S. Rykoff, Salvador Salazar-Albornoz, Mara Salvato, Lado Samushia, Ariel G. Sánchez, Basílio Santiago, Conor Sayres, Ricardo P. Schiavon, David J. Schlegel, Sarah J. Schmidt, Donald P. Schneider, Mathias Schultheis, Axel D. Schwope, C. G. Scóccola, Caroline Scott, Kris Sellgren, Hee-Jong Seo, Aldo Serenelli, Neville Shane, Yue Shen, Matthew Shetrone, Yiping Shu, V. Silva Aguirre, Thirupathi Sivarani, M. F. Skrutskie, Anže Slosar, Verne V. Smith, Flávia Sobreira, Diogo

Souto, Keivan G. Stassun, Matthias Steinmetz, Dennis Stello, Michael A. Strauss, Alina Streblyanska, Nao Suzuki, Molly E. C. Swanson, Jonathan C. Tan, Jamie Tayar, Ryan C. Terrien, Aniruddha R. Thakar, Daniel Thomas, Neil Thomas, Benjamin A. Thompson, Jeremy L. Tinker, Rita Tojeiro, Nicholas W. Troup, Mariana Vargas-Magaña, Jose A. Vazquez, Licia Verde, Matteo Viel, Nicole P. Vogt, David A. Wake, Ji Wang, Benjamin A. Weaver, David H. Weinberg, Benjamin J. Weiner, Martin White, John C. Wilson, John P. Wisniewski, W. M. Wood-Vasey, Christophe Ye'che, Donald G. York, Nadia L. Zakamska, O. Zamora, Gail Zasowski, Idit Zehavi, Gong-Bo Zhao, Zheng Zheng, Xu Zhou (), Zhimin Zhou (), Hu Zou (), and Guangtun Zhu. THE ELEVENTH AND TWELFTH DATA RELEASES OF THE SLOAN DIGITAL SKY SURVEY: FINAL DATA FROM SDSS-III. *ApJS*, 219(1):12, jul 2015. ISSN 1538-4365. doi: 10.1088/0067-0049/219/1/12. URL `http://adsabs.harvard.edu/abs/2015arXiv150100963A` `http://stacks.iop.org/0067-0049/219/i=1/a=12?key=crossref.9b82c10044d9c570d778627`

Steven W. Allen, August E. Evrard, and Adam B. Mantz. Cosmological Parameters from Observations of Galaxy Clusters. *Annu. Rev. Astron. Astrophys.*, 49(1):409–470, sep 2011. ISSN 0066-4146. doi: 10.1146/annurev-astro-081710-102514. URL `http://adsabs.harvard.edu/abs/2011ARA&A..49..409A`.

James Annis, Marcelle Soares-Santos, Michael A. Strauss, Andrew C. Becker, Scott Dodelson, Xiaohui Fan, James E. Gunn, Jiangang Hao, Željko Ivezić, Sebastian Jester, Linhua Jiang, David E. Johnston, Jeffrey M. Kubo, Hubert Lampeitl, Huan Lin, Robert H. Lupton, Gajus Miknaitis, Hee-Jong Seo, Melanie Simet, and Brian Yanny. THE SLOAN DIGITAL SKY SURVEY COADD: 275 deg 2 OF DEEP SLOAN DIGITAL SKY SURVEY IMAGING ON STRIPE 82. *ApJ*, 794(2):120, sep 2014. ISSN 1538-4357. doi: 10.1088/0004-637X/794/2/120. URL `http://adsabs.harvard.edu/abs/2014ApJ...794..120A`.

Timothy C. Beers, Kevin Flynn, and Karl Gebhardt. Measures of location and scale for velocities in clusters of galaxies - A robust approach. *AJ*, 100:32, jul 1990. ISSN 00046256. doi: 10.1086/115487. URL http://adsabs.harvard.edu/abs/1990AJ....100...32B.

Peter S. Behroozi, Risa H. Wechsler, and Hao-Yi Wu. THE ROCKSTAR PHASE-SPACE TEMPORAL HALO FINDER AND THE VELOCITY OFFSETS OF CLUSTER CORES. *ApJ*, 762(2):109, jan 2013. ISSN 0004-637X. doi: 10.1088/0004-637X/762/2/109. URL http://adsabs.harvard.edu/abs/2013ApJ...762..109B.

Michael R. Blanton, Julianne Dalcanton, Daniel Eisenstein, Jon Loveday, Michael A. Strauss, Mark SubbaRao, David H. Weinberg, John E. Anderson, Jr., James Annis, Neta A. Bahcall, Mariangela Bernardi, J. Brinkmann, Robert J. Brunner, Scott Burles, Larry Carey, Francisco J. Castander, Andrew J. Connolly, István Csabai, Mamoru Doi, Douglas Finkbeiner, Scott Friedman, Joshua A. Frieman, Masataka Fukugita, James E. Gunn, G. S. Hennessy, Robert B. Hindsley, David W. Hogg, Takashi Ichikawa, Željko Ivezić, Stephen Kent, G. R. Knapp, D. Q. Lamb, R. French Leger, Daniel C. Long, Robert H. Lupton, Timothy A. McKay, Avery Meiksin, Aronne Merelli, Jeffrey A. Munn, Vijay Narayanan, Matt Newcomb, R. C. Nichol, Sadanori Okamura, Russell Owen, Jeffrey R. Pier, Adrian Pope, Marc Postman, Thomas Quinn, Constance M. Rockosi, David J. Schlegel, Donald P. Schneider, Kazuhiro Shimasaku, Walter A. Siegmund, Stephen Smee, Yehuda Snir, Chris Stoughton, Christopher Stubbs, Alexander S. Szalay, Gyula P. Szokoly, Aniruddha R. Thakar, Christy Tremonti, Douglas L. Tucker, Alan Uomoto, Dan Vanden Berk, Michael S. Vogeley, Patrick Waddell, Brian Yanny, Naoki Yasuda, and Donald G. York. The Luminosity Function of Galaxies in SDSS Commissioning Data. *AJ*, 121(5):2358–2380, may 2001. ISSN 00046256. doi: 10.1086/320405. URL

http://stacks.iop.org/1538-3881/121/i=5/a=2358.

S. Bocquet, A. Saro, J. J. Mohr, K. A. Aird, M. L. N. Ashby, M. Bautz, M. Bayliss, G. Bazin, B. A. Benson, L. E. Bleem, M. Brodwin, J. E. Carlstrom, C. L. Chang, I. Chiu, H. M. Cho, A. Clocchiatti, T. M. Crawford, A. T. Crites, S. Desai, T. de Haan, J. P. Dietrich, M. A. Dobbs, R. J. Foley, W. R. Forman, D. Gangkofner, E. M. George, M. D. Gladders, A. H. Gonzalez, N. W. Halverson, C. Hennig, J. Hlavacek-Larrondo, G. P. Holder, W. L. Holzapfel, J. D. Hrubes, C. Jones, R. Keisler, L. Knox, A. T. Lee, E. M. Leitch, J. Liu, M. Lueker, D. Luong-Van, D. P. Marrone, M. McDonald, J. J. McMahon, S. S. Meyer, L. Mocanu, S. S. Murray, S. Padin, C. Pryke, C. L. Reichardt, A. Rest, J. Ruel, J. E. Ruhl, B. R. Saliwanchik, J. T. Sayre, K. K. Schaffer, E. Shirokoff, H. G. Spieler, B. Stalder, S. A. Stanford, Z. Staniszewski, A. A. Stark, K. Story, C. W. Stubbs, K. Vanderlinde, J. D. Vieira, A. Vikhlinin, R. Williamson, O. Zahn, and A. Zenteno. MASS CALIBRATION AND COSMOLOGICAL ANALYSIS OF THE SPT-SZ GALAXY CLUSTER SAMPLE USING VELOCITY DISPERSION σ v AND X-RAY Y X MEASUREMENTS. *ApJ*, 799(2): 214, jan 2015. ISSN 1538-4357. doi: 10.1088/0004-637X/799/2/214. URL http://adsabs.harvard.edu/abs/2015ApJ...799..214B.

J. R. Bond, G. Efstathiou, P. M. Lubin, and P. R. Meinhold. Cosmic-structure constraints from a one-degree microwave-background anisotropy experiment. *Phys. Rev. Lett.*, 66(17):2179–2182, apr 1991. ISSN 0031-9007. doi: 10.1103/PhysRevLett.66.2179. URL http://adsabs.harvard.edu/abs/1991PhRvL..66.2179B.

J. E. Carlstrom, P. A. R. Ade, K. A. Aird, B. A. Benson, L. E. Bleem, S. Busetti, C. L. Chang, E. Chauvin, H.-M. Cho, T. M. Crawford, A. T. Crites, M. A. Dobbs, N. W. Halverson, S. Heimsath, W. L. Holzapfel, J. D. Hrubes, M. Joy,

R. Keisler, T. M. Lanting, A. T. Lee, E. M. Leitch, J. Leong, W. Lu, M. Lueker, D. Luong-Van, J. J. McMahon, J. Mehl, S. S. Meyer, J. J. Mohr, T. E. Montroy, S. Padin, T. Plagge, C. Pryke, J. E. Ruhl, K. K. Schaffer, D. Schwan, E. Shirokoff, H. G. Spieler, Z. Staniszewski, A. A. Stark, C. Tucker, K. Vanderlinde, J. D. Vieira, and R. Williamson. The 10 Meter South Pole Telescope. *PASP*, 123(903):568–581, may 2011. ISSN 00046280. doi: 10.1086/659879. URL `http://adsabs.harvard.edu/abs/2011PASP..123..568C`.

John E. Carlstrom, Gilbert P. Holder, and Erik D. Reese. Cosmology with the Sunyaev-Zeldovich Effect. *Annu. Rev. Astron. Astrophys.*, 40(1):643–680, sep 2002. ISSN 0066-4146. doi: 10.1146/annurev.astro.40.060401.093803. URL `http://adsabs.harvard.edu/abs/2002ARA%26A..40..643C`.

Gilles Chabrier. Galactic Stellar and Substellar Initial Mass Function. *PASP*, 115(809):763–795, jul 2003. ISSN 0004-6280. doi: 10.1086/376392. URL `http://www.jstor.org/stable/10.1086/376392`.

M. Crocce, S. Pueblas, and R. Scoccimarro. Transients from initial conditions in cosmological simulations. *MNRAS*, 373(1):369–381, nov 2006. ISSN 0035-8711. doi: 10.1111/j.1365-2966.2006.11040.x. URL `http://adsabs.harvard.edu/abs/2006MNRAS.373..369C`.

Daniel J. Eisenstein, Idit Zehavi, David W. Hogg, Roman Scoccimarro, Michael R. Blanton, Robert C. Nichol, Ryan Scranton, HeeJong Seo, Max Tegmark, Zheng Zheng, Scott F. Anderson, Jim Annis, Neta Bahcall, Jon Brinkmann, Scott Burles, Francisco J. Castander, Andrew Connolly, Istvan Csabai, Mamoru Doi, Masataka Fukugita, Joshua A. Frieman, Karl Glazebrook, James E. Gunn, John S. Hendry, Gregory Hennessy, Zeljko Ivezić, Stephen Kent, Gillian R. Knapp, Huan Lin, YeongShang Loh, Robert H. Lupton, Bruce Margon, Timothy A. McKay, Avery Meiksin, Jeffery A. Munn, Adrian Pope, Michael W. Richmond, David

Schlegel, Donald P. Schneider, Kazuhiro Shimasaku, Christopher Stoughton, Michael A. Strauss, Mark SubbaRao, Alexander S. Szalay, Istvan Szapudi, Douglas L. Tucker, Brian Yanny, and Donald G. York. Detection of the Baryon Acoustic Peak in the LargeScale Correlation Function of SDSS Luminous Red Galaxies. *ApJ*, 633(2):560–574, nov 2005. ISSN 0004-637X. doi: 10.1086/466512. URL http://adsabs.harvard.edu/abs/2005ApJ...633..560E.

A. E. Evrard, J. Bialek, M. Busha, M. White, S. Habib, K. Heitmann, M. Warren, E. Rasia, G. Tormen, L. Moscardini, C. Power, A. R. Jenkins, L. Gao, C. S. Frenk, V. Springel, S. D. M. White, and J. Diemand. Virial Scaling of Massive Dark Matter Halos: Why Clusters Prefer a High Normalization Cosmology. *ApJ*, 672(1):122–137, jan 2008. ISSN 0004-637X. doi: 10.1086/521616. URL http://adsabs.harvard.edu/abs/2008ApJ...672..122E.

Daniel Foreman-Mackey, David W. Hogg, Dustin Lang, and Jonathan Goodman. emcee : The MCMC Hammer. *PASP*, 125(925):306–312, mar 2013. ISSN 00046280. doi: 10.1086/670067. URL http://adsabs.harvard.edu/abs/2013PASP..125..306F.

J. R. III Gott and M. J. Rees. A theory of galaxy formation and clustering. *A&A*, 45:365–376, 1975. URL http://adsabs.harvard.edu/abs/1975A%26A....45..365G.

G. J. Hill, K. Gebhardt, E. Komatsu, N. Drory, P. J. MacQueen, J. Adams, G. A. Blanc, R. Koehler, M. Rafal, M. M. Roth, A. Kelz, C. Gronwall, R. Ciardullo, and D. P. Schneider. The Hobby-Eberly Telescope Dark Energy Experiment (HETDEX): Description and Early Pilot Survey Results. *Panor. Views Galaxy Form. Evol. ASP Conf. Ser.*, 399, 2008a. URL http://adsabs.harvard.edu/abs/2008ASPC..399..115H.

Gary J. Hill, Phillip J. MacQueen, Michael P. Smith, Joseph R. Tufts, Martin M.

Roth, Andreas Kelz, Joshua J. Adams, Niv Drory, Frank Grupp, Stuart I. Barnes, Guillermo A. Blanc, Jeremy D. Murphy, Werner Altmann, Gordon L. Wesley, Pedro R. Segura, John M. Good, John A. Booth, Svend-Marian Bauer, Emil Popow, John A. Goertz, Robert D. Edmonston, and Christopher P. Wilkinson. Design, construction, and performance of VIRUS-P: the prototype of a highly replicated integral-field spectrograph for HET. In Ian S. McLean and Mark M. Casali, editors, *Ground-based Airborne Instrum. Astron. II. Ed. by McLean*, volume 7014, pages 701470–701470–15, jul 2008b. doi: 10.1117/12.790235. URL http://adsabs.harvard.edu/abs/2008SPIE.7014E.231H.

Gary J. Hill, Sarah E. Tuttle, Hanshin Lee, Brian L. Vattiat, Mark E. Cornell, D. L. DePoy, Niv Drory, Maximilian H. Fabricius, Andreas Kelz, J. L. Marshall, J. D. Murphy, Travis Prochaska, Richard D. Allen, Ralf Bender, Guillermo Blanc, Taylor Chonis, Gavin Dalton, Karl Gebhardt, John Good, Dionne Haynes, Thomas Jahn, Phillip J. MacQueen, M. D. Rafal, M. M. Roth, R. D. Savage, and Jan Snigula. VIRUS: production of a massively replicated 33k fiber integral field spectrograph for the upgraded Hobby-Eberly Telescope. In Ian S. McLean, Suzanne K. Ramsay, and Hideki Takami, editors, *Ground-based Airborne Instrum. Astron. IV. Proc. SPIE*, volume 8446, page 84460N, sep 2012. doi: 10.1117/12.925434. URL http://adsabs.harvard.edu/abs/2012SPIE.8446E..0NH.

David W. Hogg, Jo Bovy, and Dustin Lang. Data analysis recipes: Fitting a model to data. aug 2010. URL http://adsabs.harvard.edu/abs/2010arXiv1008.4686H.

E. P. Hubble. Extragalactic nebulae. *ApJ*, 64:321, dec 1926. ISSN 0004-637X. doi: 10.1086/143018. URL http://adsabs.harvard.edu/abs/1926ApJ....64..321H.

Edwin Hubble and Milton L. Humason. The Velocity-Distance Relation among Extra-Galactic Nebulae. *ApJ*, 74:43, jul

1931. ISSN 0004-637X. doi: 10.1086/143323. URL http://adsabs.harvard.edu/abs/1931ApJ....74...43H.

Andreas Kelz, Thomas Jahn, D. Haynes, G. J. Hill, H. Lee, J. D. Murphy, Justus Neumann, Harald Nicklas, M. Rutowska, C. Sandin, O. Streicher, S. Tuttle, M. Fabricius, S. M. Bauer, B. Vattiat, H. Anwand, and R. Savage. VIRUS: assembly, testing and performance of 33,000 fibres for HETDEX. In Suzanne K. Ramsay, Ian S. McLean, and Hideki Takami, editors, *Proc. SPIE*, volume 9147, page 914775, jul 2014. doi: 10.1117/12.2056384. URL http://adsabs.harvard.edu/abs/2014SPIE.9147E..75K.

B. Kirk, M. Hilton, C. Cress, S. M. Crawford, J. P. Hughes, N. Battaglia, J. R. Bond, C. Burke, M. B. Gralla, A. Hajian, M. Hasselfield, A. D. Hincks, L. Infante, A. Kosowsky, T. A. Marriage, F. Menanteau, K. Moodley, M. D. Niemack, J. L. Sievers, C. Sifon, S. Wilson, E. J. Wollack, and C. Zunckel. SALT spectroscopic observations of galaxy clusters detected by ACT and a type II quasar hosted by a brightest cluster galaxy. *MNRAS*, 449 (4):4010–4026, apr 2015. ISSN 0035-8711. doi: 10.1093/mnras/stv595. URL http://adsabs.harvard.edu/abs/2015MNRAS.449.4010K.

Andrey V. Kravtsov and Stefano Borgani. Formation of Galaxy Clusters. *Annu. Rev. Astron. Astrophys.*, 50(1):353–409, 2012. ISSN 0066-4146. doi: 10.1146/annurev-astro-081811-125502. URL http://adsabs.harvard.edu/abs/2012ARA&A..50..353K.

LSST Dark Energy Science Collaboration. Large Synoptic Survey Telescope: Dark Energy Science Collaboration. *arXiv Prepr. arXiv1211.0310*, page 133, nov 2012. URL http://adsabs.harvard.edu/abs/2012arXiv1211.0310L http://arxiv.org/abs/1211.0310.

A. Mantz, S. W. Allen, D. Rapetti, and H. Ebeling. The observed growth of massive

galaxy clusters - I. Statistical methods and cosmological constraints. *MNRAS*, 406 (3):no–no, jul 2010. ISSN 00358711. doi: 10.1111/j.1365-2966.2010.16992.x. URL http://adsabs.harvard.edu/abs/2010MNRAS.406.1759M.

A. B. Mantz, S. W. Allen, R. G. Morris, R. W. Schmidt, A. von der Linden, and O. Urban. Cosmology and astrophysics from relaxed galaxy clusters - I. Sample selection. *MNRAS*, 449(1):199–219, mar 2015. ISSN 0035-8711. doi: 10.1093/mnras/stv219. URL http://adsabs.harvard.edu/abs/2015MNRAS.449..199M.

Nicolai Meinshausen. Quantile Regression Forests. *J. Mach. Learn. Res.*, 7:983–999, dec 2006. ISSN 1532-4435. URL http://dl.acm.org/citation.cfm?id=1248547.1248582.

B. Milvang-Jensen, S. Noll, C. Halliday, B. M. Poggianti, P. Jablonka, A. Aragón-Salamanca, R. P. Saglia, N. Nowak, A. von der Linden, G. De Lucia, R. Pelló, J. Moustakas, S. Poirier, S. P. Bamford, D. I. Clowe, J. J. Dalcanton, G. H. Rudnick, L. Simard, S. D. M. White, and D. Zaritsky. Spectroscopy of clusters in the ESO distant cluster survey (EDisCS). II. *A&A*, 482(2):419–449, may 2008. ISSN 0004-6361. doi: 10.1051/0004-6361:20079148. URL http://adsabs.harvard.edu/abs/2008A&A...482..419M.

E. Munari, A. Biviano, S. Borgani, G. Murante, and D. Fabjan. The relation between velocity dispersion and mass in simulated clusters of galaxies: dependence on the tracer and the baryonic physics. *MNRAS*, 430(4): 2638–2649, feb 2013. ISSN 0035-8711. doi: 10.1093/mnras/stt049. URL http://adsabs.harvard.edu/abs/2013MNRAS.430.2638M.

S.G. Murray, C. Power, and A.S.G. Robotham. HMFcalc: An online tool for calculating dark matter halo mass functions. *Astron. Comput.*, 3-4:23–34, nov 2013. ISSN 22131337. doi: 10.1016/j.ascom.2013.11.001. URL http://adsabs.harvard.edu/abs/2013A%26C.....3...23M.

Radford M Neal. Markov Chain Monte Carlo Methods Based on 'Slicing' the Density Function. Technical report, Department of Statistics, University of Toronto, Toronto, 1997.

Michelle Ntampaka, Hy Trac, Dougal J. Sutherland, Nicholas Battaglia, Barnabás Póczos, and Jeff Schneider. DYNAMICAL MASS MEASUREMENTS OF CONTAMINATED GALAXY CLUSTERS USING MACHINE LEARNING. *eprint arXiv:1509.05409*, sep 2015. URL http://adsabs.harvard.edu/abs/2015arXiv150905409N.

J. B. Oke. Absolute Spectral Energy Distributions for White Dwarfs. *ApJS*, 27:21, feb 1974. ISSN 0067-0049. doi: 10.1086/190287. URL http://adsabs.harvard.edu/abs/1974ApJS...27...21O.

Fabian Pedregosa, Gaël Varoquaux, Alexandre Gramfort, Vincent Michel, Bertrand Thirion, Olivier Grisel, Mathieu Blondel, Peter Prettenhofer, Ron Weiss, Vincent Dubourg, Jake Vanderplas, Alexandre Passos, David Cournapeau, Matthieu Brucher, Matthieu Perrot, and Édouard Duchesnay. Scikit-learn: Machine Learning in Python. *J. Mach. Learn. Res.*, 12:2825–2830, 2012. ISSN 15324435. URL http://adsabs.harvard.edu/abs/2012arXiv1201.0490P http://dl.acm.org/citation.cfm?id=2078195\nhttp://arxiv.org/abs/1201.0490.

Planck Collaboration. Planck 2013 results. XX. Cosmology from Sunyaev-Zeldovich cluster counts. *A&A*, 571:19, oct 2013. ISSN 14320746. doi: 10.1051/0004-6361/201321521. URL http://adsabs.harvard.edu/abs/2014A&A...571A..20P http://arxiv.org/abs/1303.5080.

William H. Press and Paul Schechter. Formation of Galaxies and Clusters of Galaxies by Self-Similar Gravitational Condensation. *ApJ*, 187: 425, feb 1974. ISSN 0004-637X. doi: 10.1086/152650. URL

http://adsabs.harvard.edu/abs/1974ApJ...187..425P.

Lawrence W. Ramsey, Mark T. Adams, Thomas G. Barnes III, John A. Booth, Mark E. Cornell, James R. Fowler, Niall I. Gaffney, John W. Glaspey, John M. Good, Gary J. Hill, Philip W. Kelton, Victor L. Krabbendam, Larry E. Long, Phillip J. MacQueen, Frank B. Ray, Randall L. Ricklefs, J. Sage, Thomas A. Sebring, William J. Spiesman, and M. Steiner. Early performance and present status of the Hobby-Eberly Telescope. In *Proc. SPIE*, volume 3352, pages 34–42, 1998. doi: 10.1117/12.319287. URL http://adsabs.harvard.edu/abs/1998SPIE.3352...34R http://proceedings.spiedigitallibrary.org/proceeding.aspx?articleid=945060.

Rachel M. Reddick, Risa H. Wechsler, Jeremy L. Tinker, and Peter S. Behroozi. THE CONNECTION BETWEEN GALAXIES AND DARK MATTER STRUCTURES IN THE LOCAL UNIVERSE. *ApJ*, 771(1):30, jul 2013. ISSN 0004-637X. doi: 10.1088/0004-637X/771/1/30. URL http://adsabs.harvard.edu/abs/2013ApJ...771...30R.

A. S. G. Robotham, P. Norberg, S. P. Driver, I. K. Baldry, S. P. Bamford, A. M. Hopkins, J. Liske, J. Loveday, A. Merson, J. A. Peacock, S. Brough, E. Cameron, C. J. Conselice, S. M. Croom, C. S. Frenk, M. Gunawardhana, D. T. Hill, D. H. Jones, L. S. Kelvin, K. Kuijken, R. C. Nichol, H. R. Parkinson, K. A. Pimbblet, S. Phillipps, C. C. Popescu, M. Prescott, R. G. Sharp, W. J. Sutherland, E. N. Taylor, D. Thomas, R. J. Tuffs, E. van Kampen, and D. Wijesinghe. Galaxy and Mass Assembly (GAMA): the GAMA galaxy group catalogue (G3Cv1). *MNRAS*, 416 (4):2640–2668, oct 2011. ISSN 00358711. doi: 10.1111/j.1365-2966.2011.19217.x. URL http://adsabs.harvard.edu/abs/2011MNRAS.416.2640R.

E. Rozo, E. S. Rykoff, J. G. Bartlett, and J.-B. Melin. redMaPPer - III. A detailed comparison of the Planck 2013 and SDSS DR8 redMaPPer cluster catalogues.

MNRAS, 450(1):592–605, apr 2015. ISSN 0035-8711. doi: 10.1093/mnras/stv605. URL http://adsabs.harvard.edu/abs/2015MNRAS.450..592R.

Eduardo Rozo, Risa H. Wechsler, Eli S. Rykoff, James T. Annis, Matthew R. Becker, August E. Evrard, Joshua a. Frieman, Sarah M. Hansen, Jiangang Hao, David E. Johnston, Benjamin P. Koester, Timothy a. McKay, Erin S. Sheldon, and David H. Weinberg. COSMOLOGICAL CONSTRAINTS FROM THE SLOAN DIGITAL SKY SURVEY MaxBCG CLUSTER CATALOG. *ApJ*, 708(1):645–660, jan 2010. ISSN 0004-637X. doi: 10.1088/0004-637X/708/1/645. URL http://adsabs.harvard.edu/abs/2010ApJ...708..645R.

Eduardo Rozo, Hao-Yi Wu, and Fabian Schmidt. STACKED WEAK LENSING MASS CALIBRATION: ESTIMATORS, SYSTEMATICS, AND IMPACT ON COSMOLOGICAL PARAMETER CONSTRAINTS. *ApJ*, 735 (2):118, jul 2011. ISSN 0004-637X. doi: 10.1088/0004-637X/735/2/118. URL http://stacks.iop.org/0004-637X/735/i=2/a=118?key=crossref.2a1979692381ea23b4bd43

J. Ruel, G. Bazin, M. Bayliss, M. Brodwin, R. J. Foley, B. Stalder, K. A. Aird, R. Armstrong, M. L. N. Ashby, M. Bautz, B. A. Benson, L. E. Bleem, S. Bocquet, J. E. Carlstrom, C. L. Chang, S. C. Chapman, H. M. Cho, A. Clocchiatti, T. M. Crawford, A. T. Crites, T. de Haan, S. Desai, M. A. Dobbs, J. P. Dudley, W. R. Forman, E. M. George, M. D. Gladders, A. H. Gonzalez, N. W. Halverson, N. L. Harrington, F. W. High, G. P. Holder, W. L. Holzapfel, J. D. Hrubes, C. Jones, M. Joy, R. Keisler, L. Knox, A. T. Lee, E. M. Leitch, J. Liu, M. Lueker, D. Luong-Van, A. Mantz, D. P. Marrone, M. McDonald, J. J. McMahon, J. Mehl, S. S. Meyer, L. Mocanu, J. J. Mohr, T. E. Montroy, S. S. Murray, T. Natoli, D. Nurgaliev, S. Padin, T. Plagge, C. Pryke, C. L. Reichardt, A. Rest, J. E. Ruhl, B. R. Saliwanchik, A. Saro, J. T. Sayre, K. K. Schaffer, L. Shaw, E. Shirokoff, J. Song, R. Šuhada, H. G. Spieler, S. A.

Stanford, Z. Staniszewski, A. A. Starsk, K. Story, C. W. Stubbs, A. van Engelen, K. Vanderlinde, J. D. Vieira, A. Vikhlinin, R. Williamson, O. Zahn, and A. Zenteno. OPTICAL SPECTROSCOPY AND VELOCITY DISPERSIONS OF GALAXY CLUSTERS FROM THE SPT-SZ SURVEY. *ApJ*, 792 (1):45, aug 2014. ISSN 1538-4357. doi: 10.1088/0004-637X/792/1/45. URL http://adsabs.harvard.edu/abs/2014ApJ...792...45R.

E. S. Rykoff, B. P. Koester, E. Rozo, J. Annis, A. E. Evrard, S. M. Hansen, J. Hao, D. E. Johnston, T. A. McKay, and R. H. Wechsler. ROBUST OPTICAL RICHNESS ESTIMATION WITH REDUCED SCATTER. *ApJ*, 746 (2):178, feb 2012. ISSN 0004-637X. doi: 10.1088/0004-637X/746/2/178. URL http://adsabs.harvard.edu/abs/2012ApJ...746..178R.

E. S. Rykoff, E. Rozo, M. T. Busha, C. E. Cunha, A. Finoguenov, A. Evrard, J. Hao, B. P. Koester, A. Leauthaud, B. Nord, M. Pierre, R. Reddick, T. Sadibekova, E. S. Sheldon, and R. H. Wechsler. redMaPPer. I. ALGORITHM AND SDSS DR8 CATALOG. *ApJ*, 785(2):104, apr 2014. ISSN 0004-637X. doi: 10.1088/0004-637X/785/2/104. URL http://adsabs.harvard.edu/abs/2014ApJ...785..104R.

Alex Saro, Joseph J. Mohr, Gurvan Bazin, and Klaus Dolag. TOWARD UNBIASED GALAXY CLUSTER MASSES FROM LINE-OF-SIGHT VELOCITY DISPERSIONS. *ApJ*, 772(1):47, jul 2013. ISSN 0004-637X. doi: 10.1088/0004-637X/772/1/47. URL http://arxiv.org/abs/1203.5708 http://adsabs.harvard.edu/abs/2013ApJ...772...47S.

Neelima Sehgal, Hy Trac, Viviana Acquaviva, Peter A. R. Ade, Paula Aguirre, Mandana Amiri, John W. Appel, L. Felipe Barrientos, Elia S. Battistelli, J. Richard Bond, Ben Brown, Bryce Burger, Jay Chervenak, Sudeep Das, Mark J. Devlin, Simon R. Dicker, W. Bertrand Doriese, Joanna Dunkley, Rolando Dünner,

Thomas Essinger-Hileman, Ryan P. Fisher, Joseph W. Fowler, Amir Hajian, Mark Halpern, Matthew Hasselfield, Carlos Hernández-Monteagudo, Gene C. Hilton, Matt Hilton, Adam D. Hincks, Renée Hlozek, David Holtz, Kevin M. Huffenberger, David H. Hughes, John P. Hughes, Leopoldo Infante, Kent D. Irwin, Andrew Jones, Jean Baptiste Juin, Jeff Klein, Arthur Kosowsky, Judy M. Lau, Michele Limon, Yen-Ting Lin, Robert H. Lupton, Tobias A. Marriage, Danica Marsden, Krista Martocci, Phil Mauskopf, Felipe Menanteau, Kavilan Moodley, Harvey Moseley, Calvin B. Netterfield, Michael D. Niemack, Michael R. Nolta, Lyman A. Page, Lucas Parker, Bruce Partridge, Beth Reid, Blake D. Sherwin, Jon Sievers, David N. Spergel, Suzanne T. Staggs, Daniel S. Swetz, Eric R. Switzer, Robert Thornton, Carole Tucker, Ryan Warne, Ed Wollack, and Yue Zhao. THE ATACAMA COSMOLOGY TELESCOPE: COSMOLOGY FROM GALAXY CLUSTERS DETECTED VIA THE SUNYAEV-ZEL'DOVICH EFFECT. *ApJ*, 732 (1):44, may 2011. ISSN 0004-637X. doi: 10.1088/0004-637X/732/1/44. URL `http://adsabs.harvard.edu/abs/2011ApJ...732...44S`.

Cristóbal Sifón, Felipe Menanteau, Matthew Hasselfield, Tobias A. Marriage, John P. Hughes, L. Felipe Barrientos, Jorge González, Leopoldo Infante, Graeme E. Addison, Andrew J. Baker, Nick Battaglia, J. Richard Bond, Devin Crichton, Sudeep Das, Mark J. Devlin, Joanna Dunkley, Rolando Dünner, Megan B. Gralla, Amir Hajian, Matt Hilton, Adam D. Hincks, Arthur B. Kosowsky, Danica Marsden, Kavilan Moodley, Michael D. Niemack, Michael R. Nolta, Lyman A. Page, Bruce Partridge, Erik D. Reese, Neelima Sehgal, Jon Sievers, David N. Spergel, Suzanne T. Staggs, Robert J. Thornton, Hy Trac, and Edward J. Wollack. THE ATACAMA COSMOLOGY TELESCOPE: DYNAMICAL MASSES AND SCALING RELATIONS FOR A SAMPLE OF MASSIVE SUNYAEV-ZEL'DOVICH EFFECT SELECTED

GALAXY CLUSTERS ,. *ApJ*, 772(1):25, jul 2013. ISSN 0004-637X. doi: 10.1088/0004-637X/772/1/25. URL http://arxiv.org/abs/1201.0991 http://stacks.iop.org/0004-637X/772/i=1/a=25?key=crossref.dbce3dfdfc137953a337663

Cristóbal Sifón, Nick Battaglia, Felipe Menanteau, Matthew Hasselfield, L. Felipe Barrientos, J. Richard Bond, Devin Crichton, Mark J. Devlin, Rolando Dünner, Matt Hilton, Adam D. Hincks, Renée Hlozek, Kevin M. Huffenberger, John P. Hughes, Leopoldo Infante, Arthur Kosowsky, Danica Marsden, Tobias A. Marriage, Kavilan Moodley, Michael D. Niemack, Lyman A. Page, David N. Spergel, Suzanne T. Staggs, Hy Trac, and Edward J. Wollack. The Atacama Cosmology Telescope: Dynamical masses for 44 SZ-selected galaxy clusters over 755 square degrees. dec 2015a. URL http://adsabs.harvard.edu/abs/2015arXiv151200910S http://arxiv.org/abs/1512.00910.

Cristóbal Sifón, Henk Hoekstra, Marcello Cacciato, Massimo Viola, Fabian Köhlinger, Remco F. J. van der Burg, David J. Sand, and Melissa L. Graham. Constraints on the alignment of galaxies in galaxy clusters from ˜14 000 spectroscopic members. *A&A*, 575:A48, feb 2015b. ISSN 0004-6361. doi: 10.1051/0004-6361/201424435. URL http://adsabs.harvard.edu/abs/2015A%26A...575A..48S.

Sinclair Smith. The Mass of the Virgo Cluster. *ApJ*, 83: 23, jan 1936. ISSN 0004-637X. doi: 10.1086/143697. URL http://adsabs.harvard.edu/abs/1936ApJ....83...23S.

Volker Springel. The cosmological simulation code gadget-2. *MNRAS*, 364(4):1105–1134, dec 2005. ISSN 1365-2966. doi: 10.1111/j.1365-2966.2005.09655.x. URL http://onlinelibrary.wiley.com/doi/10.1111/j.1365-2966.2005.09655.x/full.

R. A. Sunyaev and Ya. B. Zeldovich. The Observations of Relic Radiation as a Test of the Nature of X-Ray Radiation from the Clus-

ters of Galaxies. *Comments Astrophys. Sp. Phys.*, 4, 1972. URL http://adsabs.harvard.edu/abs/1972CoASP...4..173S.

D. S. Swetz, P. A. R. Ade, M. Amiri, J. W. Appel, E. S. Battistelli, B. Burger, J. Chervenak, M. J. Devlin, S. R. Dicker, W. B. Doriese, R. Dünner, T. Essinger-Hileman, R. P. Fisher, J. W. Fowler, M. Halpern, M. Hasselfield, G. C. Hilton, A. D. Hincks, K. D. Irwin, N. Jarosik, M. Kaul, J. Klein, J. M. Lau, M. Limon, T. A. Marriage, D. Marsden, K. Martocci, P. Mauskopf, H. Moseley, C. B. Netterfield, M. D. Niemack, M. R. Nolta, L. A. Page, L. Parker, S. T. Staggs, O. Stryzak, E. R. Switzer, R. Thornton, C. Tucker, E. Wollack, and Y. Zhao. OVERVIEW OF THE ATACAMA COSMOLOGY TELESCOPE: RECEIVER, INSTRUMENTATION, AND TELESCOPE SYSTEMS. *ApJS*, 194 (2):41, jun 2011. ISSN 0067-0049. doi: 10.1088/0067-0049/194/2/41. URL http://adsabs.harvard.edu/abs/2011ApJS..194...41S.

The Dark Energy Survey Collaboration. The Dark Energy Survey. *eprint arXiv:astro-ph/0510346*, page 42, oct 2005. URL http://adsabs.harvard.edu/abs/2005astro.ph.10346T.

Jeremy Tinker, Andrey V. Kravtsov, Anatoly Klypin, Kevork Abazajian, Michael Warren, Gustavo Yepes, Stefan Gottlöber, and Daniel E. Holz. Toward a Halo Mass Function for Precision Cosmology: The Limits of Universality. *ApJ*, 688(2):709–728, dec 2008. ISSN 0004-637X. doi: 10.1086/591439. URL http://adsabs.harvard.edu/abs/2008ApJ...688..709T.

R. F. J. van der Burg, A. Muzzin, H. Hoekstra, G. Wilson, C. Lidman, and H. K. C. Yee. A census of stellar mass in ten massive haloes at z ˜ 1 from the GCLASS Survey. *A&A*, 561:A79, jan 2014. ISSN 0004-6361. doi: 10.1051/0004-6361/201322771. URL http://adsabs.harvard.edu/abs/2014A%26A...561A..79V.

K. Vanderlinde, T. M. Crawford, T. de Haan, J. P. Dudley, L. Shaw, P. A. R.

Ade, K. A. Aird, B. A. Benson, L. E. Bleem, M. Brodwin, J. E. Carlstrom, C. L. Chang, A. T. Crites, S. Desai, M. A. Dobbs, R. J. Foley, E. M. George, M. D. Gladders, N. R. Hall, N. W. Halverson, F. W. High, G. P. Holder, W. L. Holzapfel, J. D. Hrubes, M. Joy, R. Keisler, L. Knox, A. T. Lee, E. M. Leitch, A. Loehr, M. Lueker, D. P. Marrone, J. J. McMahon, J. Mehl, S. S. Meyer, J. J. Mohr, T. E. Montroy, C.-C. Ngeow, S. Padin, T. Plagge, C. Pryke, C. L. Reichardt, A. Rest, J. Ruel, J. E. Ruhl, K. K. Schaffer, E. Shirokoff, J. Song, H. G. Spieler, B. Stalder, Z. Staniszewski, A. A. Stark, C. W. Stubbs, A. van Engelen, J. D. Vieira, R. Williamson, Y. Yang, O. Zahn, and A. Zenteno. GALAXY CLUSTERS SELECTED WITH THE SUNYAEV-ZEL'DOVICH EFFECT FROM 2008 SOUTH POLE TELESCOPE OBSERVATIONS. *ApJ*, 722 (2):1180–1196, oct 2010. ISSN 0004-637X. doi: 10.1088/0004-637X/722/2/1180. URL `http://adsabs.harvard.edu/abs/2010ApJ...722.1180V`.

Matthew G. Walker, Mario Mateo, Edward W. Olszewski, Rebecca Bernstein, Xiao Wang, and Michael Woodroofe. Internal Kinematics of the Fornax Dwarf Spheroidal Galaxy. *AJ*, 131(4):2114–2139, apr 2006. ISSN 0004-6256. doi: 10.1086/500193. URL `http://adsabs.harvard.edu/abs/2006AJ....131.2114W`.

David H. Weinberg, Michael J. Mortonson, Daniel J. Eisenstein, Christopher Hirata, Adam G. Riess, and Eduardo Rozo. Observational probes of cosmic acceleration. *Phys. Rep.*, 530(2):87–255, sep 2013. ISSN 03701573. doi: 10.1016/j.physrep.2013.05.001. URL `http://adsabs.harvard.edu/abs/2013PhR...530...87W`.

S. D. M. White and M. J. Rees. Core condensation in heavy halos - A two-stage theory for galaxy formation and clustering. *MNRAS*, 183:341–358, 1978. URL `http://adsabs.harvard.edu/abs/1978MNRAS.183..341W`.

F. Zwicky. Die Rotverschiebung von extragalaktischen Nebeln. *Helv. Phys. Acta*, 6: 110–127, 1933. URL `http://adsabs.harvard.edu/abs/1933AcHPh...6..110Z`.